Geomorphology 327 (2019) 93–110

Contents lists available at ScienceDirect

Geomorphology

journal homepage: www.elsevier.com/locate/geomorph

Explaining artificial side channel dynamics using data analysis and model calculations

R. Pepijn van Denderen[a,*], Ralph M.J. Schielen[a,b], Sam G. Westerhof[a,b], Susanne Quartel[b], Suzanne J.M.H. Hulscher[a]

[a] Water Engineering & Management, Faculty of Engineering Technology, University of Twente, The Netherlands
[b] Ministry of Infrastructure and Water Management-Rijkswaterstaat, The Netherlands

ARTICLE INFO

Article history:
Received 31 May 2018
Received in revised form 19 October 2018
Accepted 19 October 2018
Available online 25 October 2018

Keywords:
Side channel
Artificial side channel
Bifurcation
Bifurcation sediment sorting
Floodplain sedimentation
River morphodynamics

ABSTRACT

Side channel construction is a common intervention to increase both flood safety and the ecological value of the river. Three side channels of Gameren in the river Waal (The Netherlands) show amounts of large aggradation. We use bed level measurements and grain size samples to characterize the development of the side channels. We relate the bed level changes and the deposited sediment in the side channels to the results of hydrodynamic computations. Two of the three side channels filled mainly with suspended bed-material load. In one of these channels, the bed level increased enough that vegetation has grown and fine suspended load has settled. In the third side channel, the bed shear stresses are much smaller and, in addition to the suspended bed-material load, fine sediment settles. Based on the side channel system at Gameren, we identify two types of side channels: one type fills predominantly with suspended bed-material load from the main channel and a second type fills predominantly with fine suspended load. This gives an indication of the main mechanisms that lead to the aggradation in artificial side channel systems.

1. Introduction

Side channels are man-made or natural secondary channels that convey considerably less discharge compared to the main channel and are connected to the main channel at their upstream and downstream ends. In many regulated rivers, side channels disappeared due to human interventions (e.g., Hohensinner et al., 2014) and currently, side channels are (re)constructed to, for example, increase the discharge capacity during peak flows (Simons et al., 2001; Nabet, 2014) or to restore the river to a more natural state (Schiemer et al., 1999; Formann et al., 2007; Riquier et al., 2015; Van Dyke, 2016). In side channels, which are constructed to increase the discharge capacity, aggradation is undesired. The aim of this paper is to get a better insight into the morphodynamic development of artificial side channels after construction.

Natural side channels can form in rivers, for example, as meander cutoffs or in anabranching rivers. Bed level changes in side channels are generally caused by a mismatch between the sediment supply and the transport capacity of the channel. In meander cutoffs, the downstream channels generally differ in length. This usually results in a steeper water surface gradient over the shorter channel leading to a relatively larger discharge conveyance and thereby transport capacity compared to the longer channel (Mendoza et al., 2016; Van Denderen et al., 2018a). The longer channel therefore starts to aggrade (Constantine et al., 2010; Dieras et al., 2013; Zinger et al., 2013; Van Denderen et al., 2018a). A plugbar can form if the transport capacity in the aggrading channel is much smaller than the supply (Constantine et al., 2010; Toonen et al., 2012; Kleinhans et al., 2013). Channels that receive a limited amount of bedload sediment due to, for example, a plugbar or a log jam are then slowly filled with finer sediment that is supplied to the channel during overbank flow conditions (Makaske et al., 2002; Constantine et al., 2010; Toonen et al., 2012). If the channel is still connected to the main channel at the downstream end, backflow can occur in the side channel leading to aggradation even during base flow conditions (Citterio and Piégay, 2009; Riquier et al., 2017). Channels without a blockage at the upstream entrance show deposition of coarse sediment that is spread over the channel until a certain bed level is reached after which fine sediment can be deposited (Makaske et al., 2002; Dieras et al., 2013).

The sediment supply to the downstream channels is function of local flow patterns and bed slope effects at the bifurcation (Bulle, 1926; Bolla Pittaluga et al., 2003; Kleinhans et al., 2008; Kleinhans et al., 2013; Dutta et al., 2017; Van Denderen et al., 2018a). Large bifurcation angles and spiral flow at the bifurcation, due to the presence of an upstream river bend, can create a secondary flow over the cross section. This

* Corresponding author.
E-mail address: r.p.vandenderen@utwente.nl (R. Pepijn van Denderen).

https://doi.org/10.1016/j.geomorph.2018.10.016
0169-555X/

leads to near-bed flow velocities that direct more sediment towards the bifurcating channel or the channel in the inner bend (Kleinhans et al., 2008, 2012; Dutta et al., 2017). Bed slope effects at the bifurcation add a gravity component to the bedload transport direction that can divert sediment from a channel with a higher bed level towards a channel with a lower bed level (Bolla Pittaluga et al., 2003). Smaller particles go up a slope more easily than larger particles (Parker and Andrews, 1985) and this results a sediment supply that is finer to the channel with a higher bed level than the one with a lower bed level. Both the secondary flow and the bed slope mainly affect sediment transported as bedload and much less the sediment in suspension, and hence both processes can cause differences in grain size of the sediment supply to the downstream channels.

Artificial side channels, at least those in the Netherlands, are often limited in their discharge conveyance for their effect on the navigational function of the river (Simons et al., 2001). A large discharge withdrawal from the main channel can cause side currents and aggradation in the main channel, and might therefore hinder the navigational function of the main channel. For that reason, the discharge withdrawal from the main channel is in the Netherlands limited to 3–5% of the total discharge during bankfull flow conditions (Akkerman, 1993; Mosselman, 2001; Jans, 2004). This is achieved by constructing weirs or culverts (Simons et al., 2001) that likely affect the sediment supply and transport capacity of the side channels. In addition, the Dutch side channels are often constructed in between groynes that affect the flow field at the bifurcation and confluence. In general, the bed level in between groynes varies as a function of an import of sediment during peak flows (Yossef, 2005) and an export of sediment by navigation-induced currents (Ten Brinke et al., 2004). The sediment that is brought into suspension due to these currents might be supplied to the side channel. The large bed level gradient that occurs between the main channel and the groyne field likely reduces the sediment supply towards the side channel. These structures complicate the sediment dynamics at the bifurcation and confluence of the side channel system.

Most of the artificial side channels in the Netherlands show aggradation. It is unknown how fast and with which type of sediment these side channels aggrade. Maintenance efforts are therefore difficult to plan. The objective of this paper is to observe and explain the characteristics of the deposited sediment and the physical processes behind the bed level changes of a side channel system at Gameren in the river Waal. We first give an overview of the hydrodynamic and morphodynamic characteristics of the river Waal and the side channel system of Gameren (Section 2). We measured the bed level and collected grain size samples in the three channels (Section 3) to study the aggradation rate and the type of sediment that is deposited inside the three side channels. In addition, we set up a hydrodynamic model of the side channel system at Gameren to estimate the bed shear stresses in the side channels. We relate the bed level changes and the grain sizes in the side channels to the results of a hydrodynamic model (Section 4). We use these three channels to characterize the development of side channels (Section 5).

2. Description of the side channel system

More than 20 side channels have been constructed in the Dutch Rhine branches to reduce the water levels during peak flow and to increase the ecological value of the river (Simons et al., 2001; Baptist and Mosselman, 2002). One of these side channel systems is located near Gameren in the floodplain of the river Waal. A system of three side channels was constructed between 1996 and 1999 (Fig. 1). The side channels were constructed to compensate for a dike relocation that reduced floodplain width. The East and the West channel were dug in 1996 and the Large channel was created in 1999. Since their construction, the side channels have been aggrading.

2.1. Characteristics of the river Waal

The river Waal is one of the Rhine branches and flows from the Pannerdensche Kop to the Merwede Kop (Fig. 1). The average annual discharge is about 1500 m^3/s, floodplains start to become inundated at 2900 m^3/s and the 10-yr flood (a peak discharge of an annual 0.1 probability) is about 6100 m^3/s (Hegnauer et al., 2014). The yearly average sediment transport in the river Waal is about 200,000 m^3/yr for sand (0.063–2 mm) and about 550,000 m^3/yr for fine sediment ($\leq$0.063 mm) (Frings et al., 2015). Discharge measurements at Tiel in the river Waal show that in the first eight years after the construction of the first two channels (1996) two 10-yr floods occurred (Fig. 2). After 2003, peak flows larger than 5300 m^3/s (5-yr flood) are much less frequent.

The morphological conditions vary over the river Waal. The bed level in the river Waal decreases on average between 1 and 2 cm each year due to a shortage of the sediment supply from upstream (Sieben, 2009). The D_{50} in the top layer of the bed in the main channel of the river Waal decreases from 2.46 mm just downstream of the Pannerdensche Kop (river kilometer (rkm) 858) to 0.5 mm just upstream of the Merwede Kop (rkm 952) (Fig. 3). In between the Pannerdensche Kop and the Merwede Kop, the D_{50} of the bed material decreases on average by about 0.8% per kilometer (Ten Brinke, 1997; Frings, 2007), but the variation over the width and length of the river is large (Fig. 3B). At Gameren (rkm 936–939) the average D_{50} of the bed material in the main channel is 0.75 mm (Ten Brinke, 1997). The grain size of the suspended bed-material load was measured during peak flows in 1998 for the Pannerdensche Kop and in 2004 for the Merwede Kop (Fig. 3). The width averaged sieve curve was averaged over samples from 0.2 m, 0.5 m and 1 m above the river bed and the samples were collected using a mesh size of 50 μm (Frings, 2007; Frings and Kleinhans, 2008). These samples therefore mainly consisted of suspended bed-material load. While the D_{50} of the bed material decreases over the length of the river, the grain size of the suspended bed-material load seems to be similar over the length of the river Waal.

During peak flows, sediment is deposited on the banks and in the floodplain of the river Waal (Sorber, 1997; Middelkoop and Asselman, 1998; Ten Brinke et al., 1998). Measurements during peak flows in 1993 and 1995 show that on average sand is deposited in the first 50–100 m of the floodplain (Middelkoop and Asselman, 1998). In the floodplain at Gameren, the peak flow of 1995 resulted in a bed level increase in the floodplain of up to 7 cm where the West and East channel currently are located (Sorber, 1997). The mean grain size of the deposited material was estimated to be ~0.3 mm (Sorber, 1997; Ten Brinke et al., 1998). This corresponds with the suspended bed-material load (Fig. 3) (Frings and Kleinhans, 2008). Farther away from the main channel, the deposited sediment in the floodplain mainly consisted of silty clay and during the peak flow in 1993 the average deposition of overbank fines ranged between 0.5 and 1.5 mm (Middelkoop and Asselman, 1998).

Several other interventions were carried out in the river Waal to reduce the risk of flooding. One of these interventions was to reduce the groyne height in the main channel. A lower groyne height leads to less friction in the main channel and therefore increases its discharge capacity. In the upper part of the river Waal (rkm 887–915), the groyne height reduction resulted in a bed level increase in the main channel of about 5 cm between 2009 and 2012 (Klop, 2015). Within the groyne fields slight degradation occurred, but this was based on limited data (Klop and Dongen, 2015). In the lower part of the river Waal (rkm 915–953), the groyne height reduction was executed between 2013 and 2014, but the morphodynamic effect has not yet been analyzed. The groyne height reduction likely reduced the bed level between the groynes at Gameren and therefore affected the bed level in the side channels because the bifurcations and confluences of the side channels at Gameren are in the groyne fields.

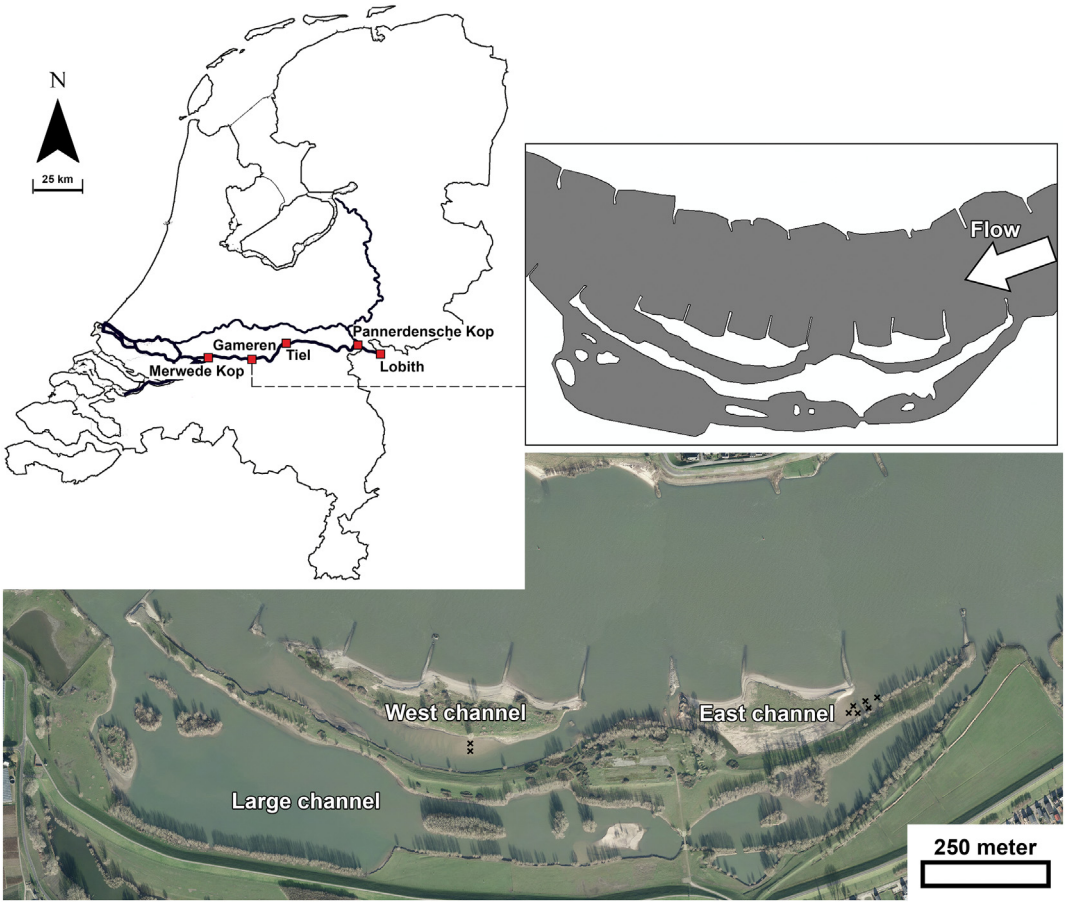

Fig. 1. Aerial images of Gameren in the floodplain of the river Waal in the Netherlands (51° 48′ 22.4″ N 5° 12′ 23.8″ E) with the three side channels and the main channel (After images of Rijkswaterstaat). The black crosses in the aerial image denote the location of the sediment cores (Fig. 14).

2.2. The side channels at Gameren

The side channels at Gameren were constructed to compensate for the water level increase due to a reduction of the floodplain width. The ecological objectives are secondary and are beyond the scope of this paper. The two small side channels were constructed in 1996 and are referred to as the *West* and *East* channel (Fig. 1). The *Large* channel was finished in 1999 and connects an old clay mining pit with the main channel. The discharge capacity in the West and East channel is limited by weirs at their entrance, and in the Large channel a bridge acts as a culvert that limits the discharge capacity. The bed level and the weir of the East channel were designed such that the channel conveys discharge on average 100 d/yr corresponding to 2200 m^3/s in the river Waal. The weir and bed level of the West channel were constructed lower such that the channel conveys discharge on average 265 d/yr corresponding to 1500 m^3/s

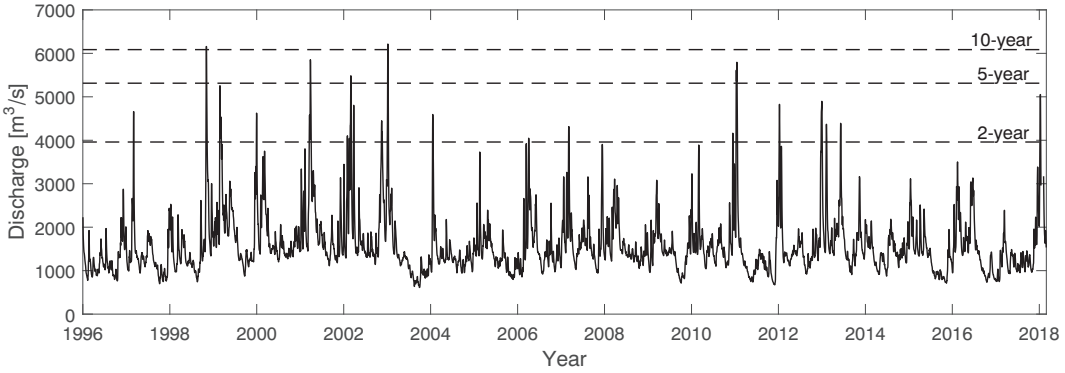

Fig. 2. The discharge at Tiel between 1996 and 2018 with the discharge levels for three return periods of flood levels (Hegnauer et al., 2014).

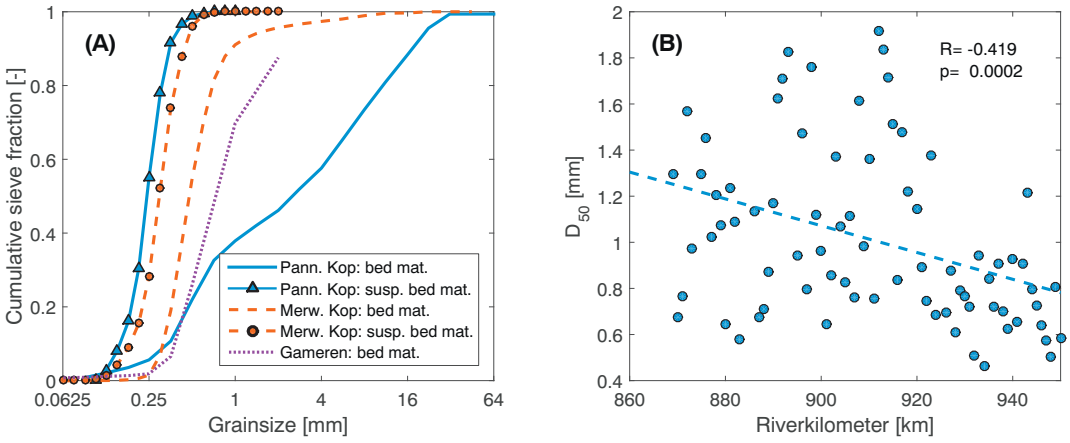

Fig. 3. The variation of the grain size over the length of the river Waal. (A) The average sieve curve of the sediment at the top of the active layer of the bed and the suspended bed material during peak flows. The peak discharge in the river Waal for the measurements at the Pannerdensche Kop and the Merwede Kop are 6173 m^3/s and 4527 m^3/s, respectively (Frings and Kleinhans, 2008). The bed material in the main channel at Gameren is averaged over the river axis (rkm 936–939) and was collected in 1995/1996 (Ten Brinke, 1997). (B) The D_{50} in the top layer of the bed on the center line of the river Waal measured in 1995/1996 (Ten Brinke, 1997). The correlation parameters (R and p) are based on the Spearman's rank correlation.

in the river Waal. The Large channel is connected with the main channel permanently. After the construction of the channels, their morphodynamic development caused the discharge conveyance and the connectivity of the side channels to change. For example, because bank erosion at the entrance of the West and the East channel, the flow is currently able to flow around the weir that was supposed to control the discharge conveyance in the channels. Between 2000 and 2002 several flow velocity measurements were carried out using an Acoustic Doppler Current Profiler (ADCP) (Jans, 2004) and from these measurements the discharge in each channel was computed (Fig. 4). Both the discharge in the West channel and the East channel seem to increase linearly with increasing discharge in the main channel. In the Large channel the trend changes for discharges larger than 3300 m^3/s, because for these discharges the water can flow around and over the bridge increasing the discharge capacity of the channel. The measurements show that during bankfull discharge conditions in the river Waal, the combined discharge in the three channels is about 5% of the total discharge in the main channel.

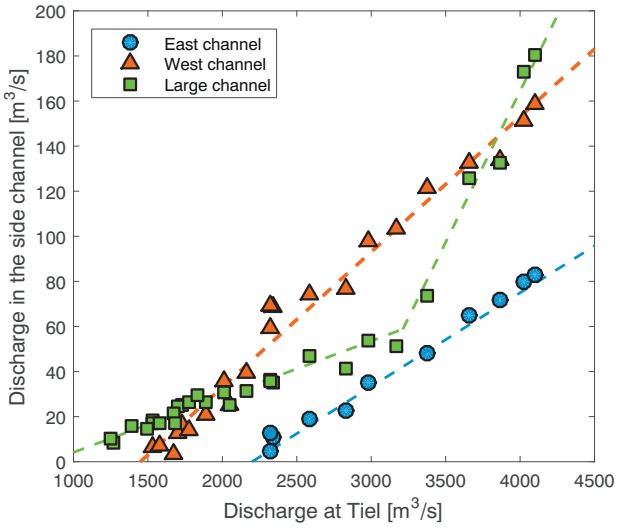

Fig. 4. The conveyance of the three side channels, measured using an ADCP between 2000 and 2002, as a function of the discharge in the main channel of the river Waal at Tiel (Jans, 2004). The dashed lines are based on a linear least square fit of the measuring points. Two lines are fitted for the Large channel one for $Q_{Tiel} \leq 3500\ m^3/s$ and one for $Q_{Tiel} > 3500\ m^3/s$.

The floodplain near Gameren is covered with a clay and sandy clay layer that reaches 6–10 m below the average bed level (Data and Information of the Dutch subsoil: https://www.dinoloket.nl). The bed of the three channels was therefore initially covered with clay and sandy-clay. Below these layers, gravel and coarse sand can be found. Until 1996, a brick factory was present in the floodplain that created a large clay pit that currently is located at the downstream end of the Large channel. It was expected that this pit would slowly fill with sediment, but this was too slow for the ecological purpose of the channel and therefore sediment was dumped in the pit in 2009 (about 500,000 m^3). A small channel was dredged from the downstream end of the Large channel to dump this sediment. Other human interventions in the system are limited to the protection of groynes, which due to bank erosion in the side channel were bypassed, the application of bank protection just downstream of the bridge in the Large channel, and the maintenance of vegetation.

Bank erosion in the side channels has been, on average, very limited. The banks mainly consist of cohesive material and therefore the bank erosion primarily occurred at locations with large flow velocities. These locations are the surrounding banks of the weirs in the West and East channels, and just downstream of the bridge in the Large channel. In addition, at the downstream end of the West channel the bank has retreated up to 40 m (Fig. 5). This region is not protected by groynes or floodplain and the bank retreat was therefore likely caused by the attack of waves from ships.

3. Methods

Fourteen bed level measuring campaigns were carried out and sediment samples were collected from the three side channels in April 2017 and from the East channel in March 2018. We estimated the hydrodynamic conditions in the side channels using a hydrodynamic model.

3.1. Bed level measurements

The bed level measurements vary in coverage and measuring method (Table 1). A dGPS (accuracy: 5 cm) was used to measure

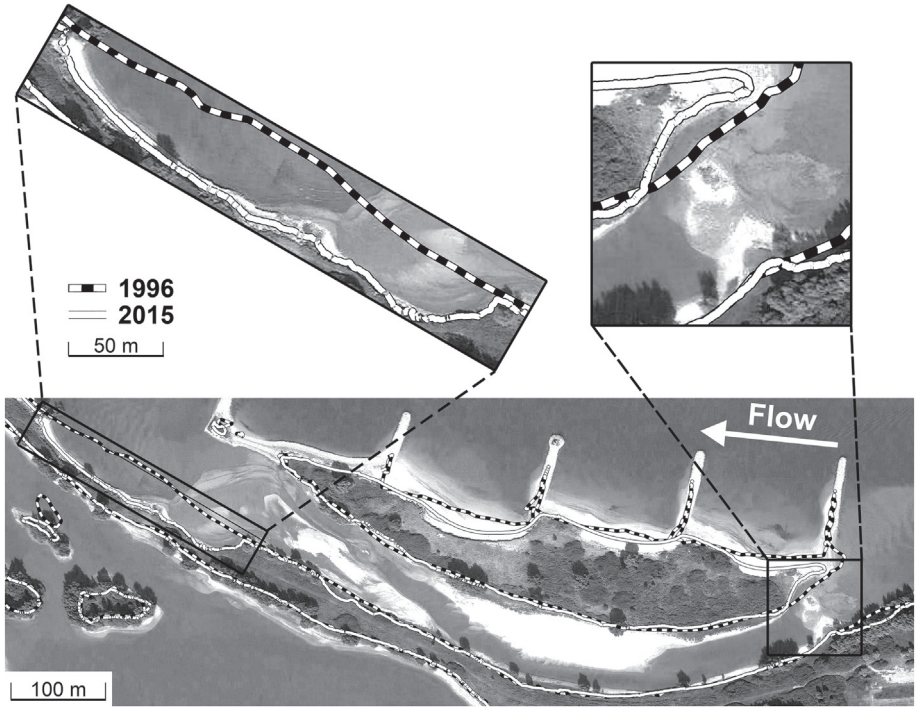

Fig. 5. Bank erosion at the bifurcation and the confluence of the West channel. The lines show the location where the bed level is 3 m +NAP (Amsterdam Ordnance Datum) in 1996 and in 2015. The background image is from 2016 (Google Earth).

the bed level above the water level surface and the shallow areas. The Large channel and deeper areas of the West channel were measured using a single-beam echo sounder (accuracy: 10–15 cm). From 2003, regular LIDAR measurements (5–10 points per m^2, accuracy: 5 cm) were carried out. These do not penetrate the water column and therefore only the bed level in the East channel was retrieved from these measurements. Most of these measurements were carried out during base flow conditions. In 2018, multi-beam measurements (accuracy: 5 cm) were carried out during a peak flow (5050 m^3/s). The largest bed level changes are expected to occur during peak flow and therefore the measured aggradation rate depends on the moment of measurement.

Table 1
A list of the available bed level data for the side channels at Gameren with the measuring technique and the data coverage.

	Date		Technique	Coverage
	December	1996	dGPS and single-beam echo sounder	East and West channel
	December	1999	dGPS and single-beam echo sounder	Full area
	November	2000	dGPS and single-beam echo sounder	Full area
	December	2001	dGPS and single-beam echo sounder	East and Large channel
	November	2002	dGPS and single-beam echo sounder	Full area
2	September	2003	LIDAR	East channel
29	February	2008	LIDAR	East channel
	October	2009	LIDAR and single-beam echo sounder	East and Large channel
17	October	2010	LIDAR	East channel
	March	2011	LIDAR	East channel
24	August	2012	LIDAR	East channel
8	September	2013	LIDAR	East channel
25	June	2014	LIDAR	East channel
15	February	2015	LIDAR	East channel
31	January	2018	Multi-beam echo sounder	Full area, excl. upstream Large channel

3.2. Grain size samples

The grain size in the side channels is expected to vary over the length and width of the channels, and to vary in time as a function of the hydrodynamic conditions. In addition, we expect that the weir at the entrance of East and West channel reduces the sediment supply to the side channel. We took sediment samples in each channel along several cross sections and in the groyne fields at the bifurcations and confluences (Fig. 12). In addition, we took three sediment cores upstream and three sediment cores downstream of the weir in the East channel (Fig. 1). These cores show the effect of the weir on the grain size that enters the side channel. It was not possible to take similar samples around the weir of the West channel because of armoring in front of the weir and large scour behind the weir. However, we took two sediment cores from the point bar in the West channel to study the variation of the grain size of the deposited sediment through the channel in time (Fig. 1).

We collected 86 sediment samples in the three side channels in April and May 2017. This was after a period of 10 months without discharges larger than 1800 m^3/s in the river Waal, suggesting a relatively calm period from morphological point of view. Large areas of the East and West channels were above the water level and in these areas, we collected the top layer of the bed with an auger. For the areas below the water level we used a Van Veen Grab sampler. After the peak flow of January 2018, we took 11 additional samples with an auger in the East channel to have an indication of the effect of peak flows on sediment deposition in the East channel. We used a dGPS to record the location of the samples and, where the water depth was less than 1 m, we also recorded the bed level.

We computed the grain size characteristics by sieving the sediment samples. We first wet sieved the samples to extract the fraction

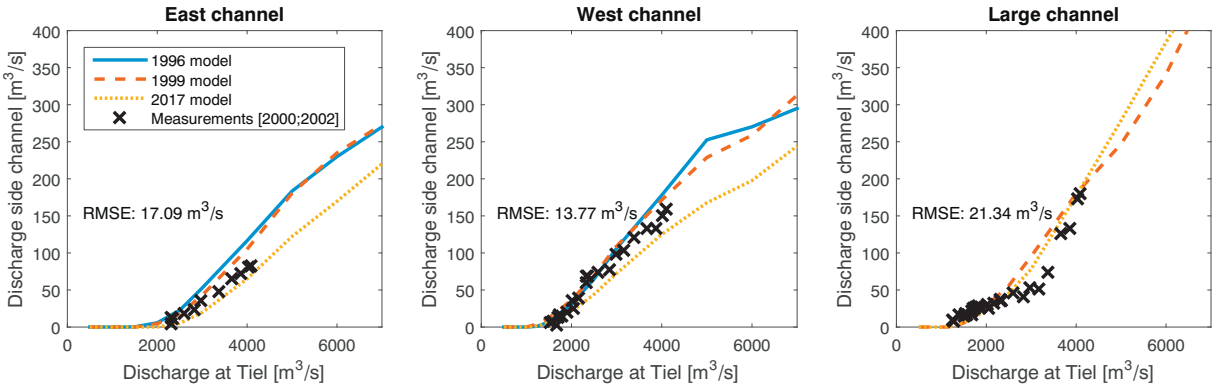

Fig. 6. A comparison of the discharge at the entrance of the three side channels from the three models and the measurements between 2000 and 2002 (Fig. 4). The root-mean-squared error (RMSE) is computed using the measurements and the 1999 model results.

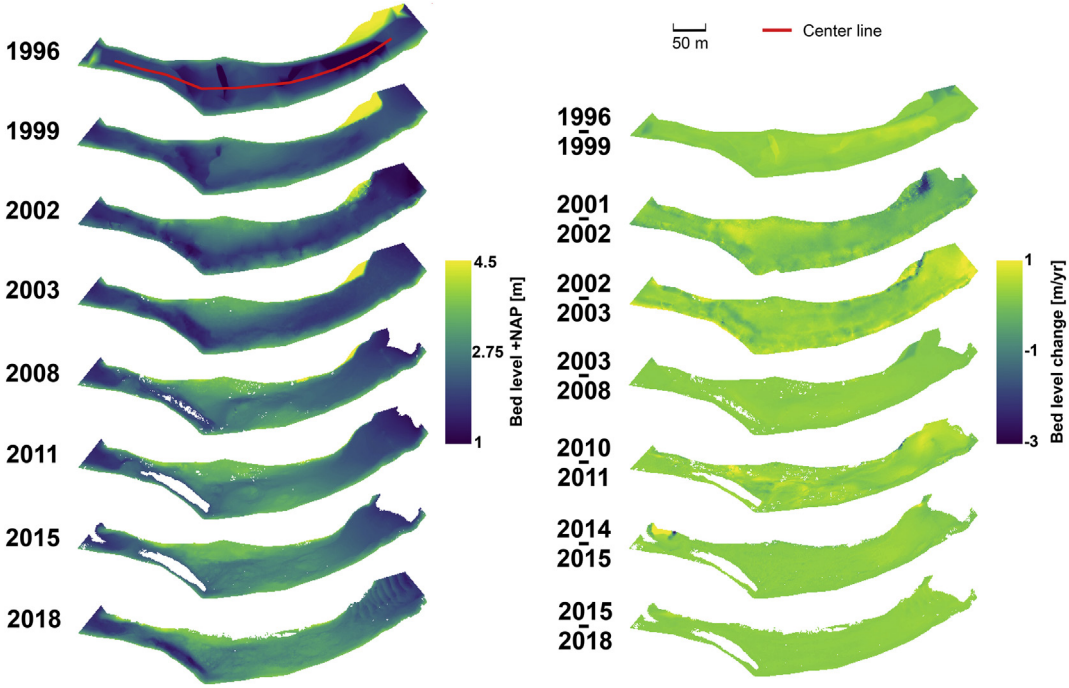

Fig. 7. Left: The bed level of the East channel relative to NAP (Amsterdam Ordnance Datum) for several years. Right: The average bed level change per year between two measurements.

<0.063 mm and the remaining material we dry sieved. The dry sieving was carried out using mesh sizes: 63, 90, 125, 150, 212, 250, 300, 500, 600, 1000, 1400 and 2000 μm. Based on the sieve results, we computed the characteristic grain sizes (D_{10}, D_{50}, D_{90}), and the silt, sand and gravel fractions. Based on these measurements, we can determine what type of sediment is deposited in the side channels

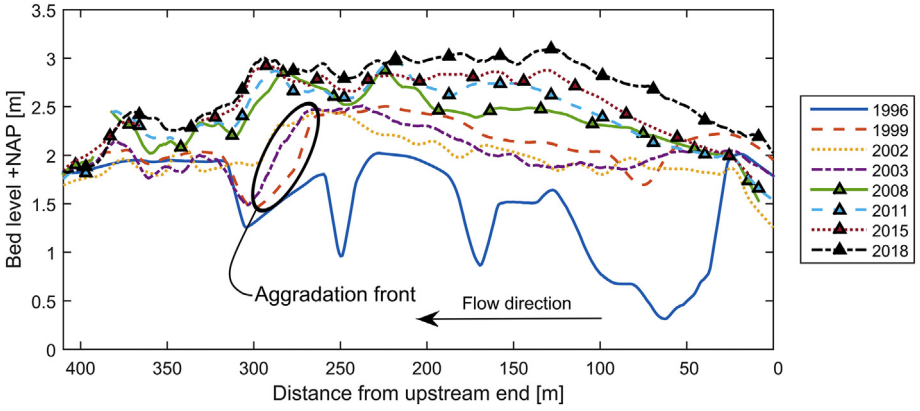

Fig. 8. The change in bed level height on the center line of the East channel (Fig. 7) filtered with a moving average over 10 m.

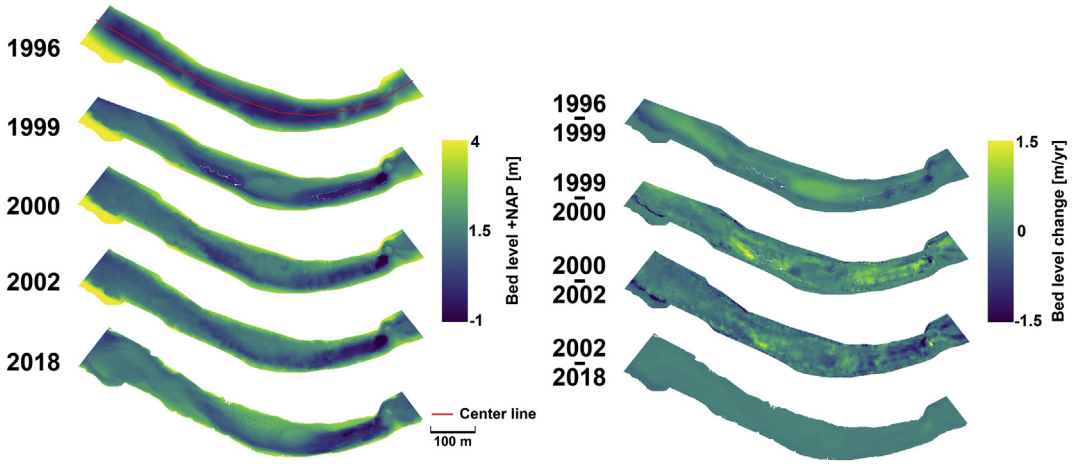

Fig. 9. Left: The bed level of the West channel relative to NAP (Amsterdam Ordnance Datum) for several years. Right: The average bed level change per year between two measurements.

and relate this to how the deposited sediment is transported in the main channel, i.e., as suspended load, as suspended bed-material load or as bedload.

3.3. Hydrodynamic model

Hydrodynamic computations were carried out using a two-dimensional depth-averaged version of the Delft3D Flexible Mesh software (Kernkamp et al., 2011). The model computes the flow velocities and the water level in the river for a given bed level, bed roughness, upstream discharge and downstream water level. The model is created based on two GIS databases of the Rhine branches that are provided by Rijkswaterstaat (Becker et al., 2014). One describes the situation in 1995 without the side channels at Gameren and one describes the situation in 2017 in which the side channels are present. From these databases we extracted the bed level and the floodplain roughness. The main channel roughness is based on a calibration of water level measurements in the main channel. We calibrated the model for three discharge levels that occurred in 1994 and 1995 such that the model gives a good estimation of the hydrodynamic conditions in the river for a range of discharge levels (Supplementary material 1).

We used the model results to calculate the discharge conveyance of the side channels, the streamlines in the floodplain and the bed shear stress in the side channels as a function of the discharge in the main channel. We apply the model to three different states of the side channels: (1) representing 1996, (2) representing 1999 and (3) representing 2017. This corresponds with the initial state of the West and East channel (1996), the initial state of the Large channel (1999), and the state during the recent grain size measurements (2017). The 1996 and the 1999 model are based on the GIS database of 1995 with the measured bed level (Section 3.1) of the side channels in 1996 and 1999, respectively. We computed the hydrodynamic conditions for twelve discharges ranging from 500 m^3/s to 7000 m^3/s using steady state boundary conditions. These discharge conditions range from base flow up to peak flow conditions.

We compare the computed discharge in the side channels with the measured discharge (Fig. 6). The discharge was measured between 2000 and 2002. The model result that is closest to these years is 1999, and we compute the error based on the 1999 results. Due to the difference in years between the measurements and the model, the error is related to the aggradation rate in the channels. This results in an overestimation of the discharge by the 1999 model. The discharge measurements in the Large channel show a change in trend due to the presence of the bridge in the channel (Fig. 4). This change in trend is not well captured by the model and this is likely caused by an incorrect representation of the culvert in the model resulting in an overestimation of the discharge between 2000 m^3/s and 4000 m^3/s. For larger discharges, the flow in the floodplain becomes more important and the effect of the bridge is smaller.

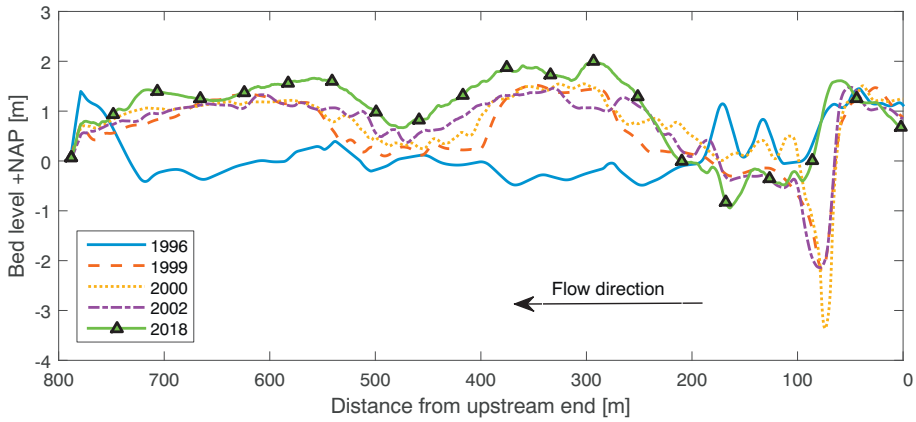

Fig. 10. The change in bed level height on the center line of the West channel (Fig. 9) filtered with a moving average over 10 m.

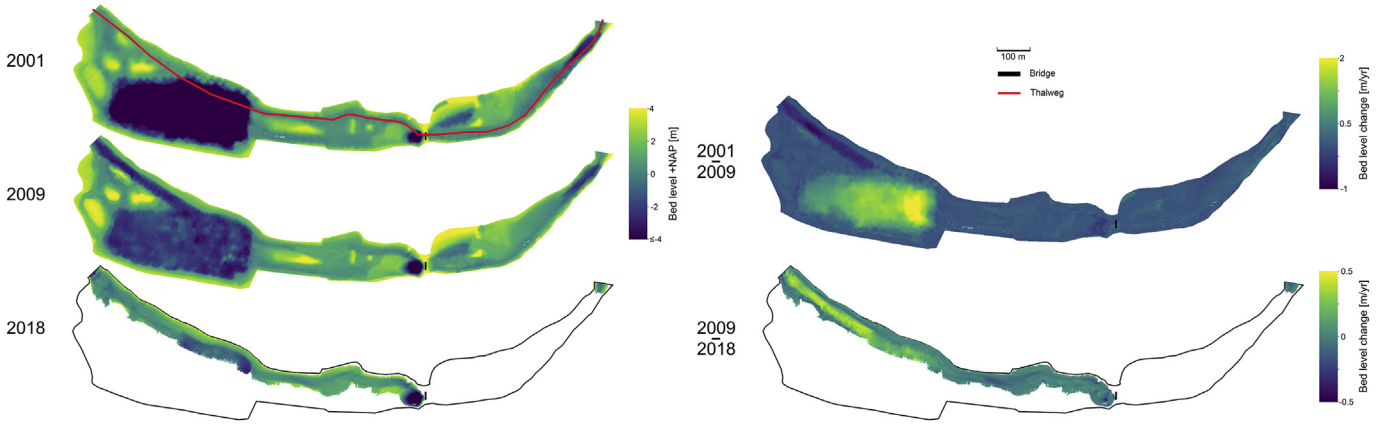

Fig. 11. Right: The bed level of the Large channel relative to NAP (Amsterdam Ordnance Datum) for several years. The dark blue areas are lower than −4 m and down to −16 m. Left: The average bed level change per year between two measurements.

3.4. Relation between the measurements and the model results

To better understand the morphodynamic development of the side channels, we relate the bed level measurements, the grain size measurements and hydrodynamic model results. The bed level measurements vary in coverage, but the center line of the East and West channel, and the thalweg of the Large channel is for most dates available. We therefore use the measured average bed level height of these longitudinal profiles and combine these with the measured grain sizes and the computed hydrodynamic conditions in the channels. We focus on the East channel, because the data of the West and Large channel is limited. The results of the other two channels are shown in the Supplementary material. We compute the correlation using the Spearman's rank correlation that, in contrast to the Pearson's correlation, does not assume a linear relation between the parameters. The correlation results in a correlation coefficient (R) and a p-value for which we assume that $p<0.01$ is sufficient to assume a correlation between the parameters. This corresponds with a false-positive probability of about 11% (Goodman, 2001; Nuzzo, 2014). In addition, we use a linear relation to show the trend of the correlation, but we immediately note that we have insufficient data to suggest any empirical relation.

4. Results and interpretation

In this section we present the bed level and grain size measurements. Next, we give an overview of the hydrodynamic results and we relate these with our measurements.

4.1. Bed level changes

4.1.1. East channel

The bed level in the East channel increased quickly after its construction in 1996 (Fig. 7). This increase in bed level was mainly caused by an aggradation front that migrated through the East channel (Fig. 8). Such an aggradation front is a bed wave that forms and migrates downstream due to a large difference between the sediment supply and the transport capacity of the channel (De Vries, 1971; Jansen et al., 1979). The point density of the bed level measurement in 2002 is too small to capture the front correctly. In 1999, the aggradation front had passed almost fully through the East channel and the bed level changes after 1999 were therefore much smaller. Apart from the aggradation front, the bed level continued to increase, but more slowly. The aggradation mainly occurred in the central part of the channel starting in the inner bend (Fig. 7). The downstream end of the side channel was initially higher compared to the rest of the channel and showed the least aggradation. The bed level measurements of 2018 were carried out during peak flow. The flow velocities during this peak flow were sufficiently high such that small dunes (height≈0.2 m; length≈10 m) formed at the entrance of the East channel (Fig. 7). This indicates that during peak flows the flow velocities are large and significant bedload transport occurs (Jansen et al., 1979).

4.1.2. West channel

The West channel aggraded initially mainly in the inner bend where a point bar formed and just downstream of the outer bend where another bar formed (Fig. 9). Initially large flow velocities at the entrance of the channel caused a large amount of scour just downstream of the weir and bank erosion that allowed the flow to circumvent the weir. The initial bed level change is large (up to 1 m/yr in the inner bend), but after 1999, the bed level changes were much smaller (Fig. 10). The initial aggradation front is not visible in the measurements, but possibly went through the channel between 1996 and 1999. After 2002, the aggradation rate is small, but the bed level continues to increase.

Table 2
An overview of the characteristic grain sizes for each channel including their groyne fields. The mean value (μ) and the standard deviation (σ) are based on a normal distribution with the number of samples (N).

	D_{10} [mm] $\mu \pm \sigma$ (N)	D_{50} [mm] $\mu \pm \sigma$ (N)	D_{90} [mm] $\mu \pm \sigma$ (N)	Silt frac. [%] $\mu \pm \sigma^a$ (N)	Sand frac. [%] $\mu \pm \sigma^a$ (N)	Gravel frac. [%] $\mu \pm \sigma^a$ (N)
West	0.19 ± 0.05 (27)	0.31 ± 0.08 (30)	0.52 ± 0.2 (28)	2.7 ± 5 (31)	94 ± 11 (31)	3.5 ± 10 (31)
East	0.14 ± 0.03 (16)	0.22 ± 0.05 (20)	0.38 ± 0.08 (19)	5.0 ± 7 (20)	94 ± 7 (20)	0.96 ± 3 (20)
Large	0.16 ± 0.07 (16)	0.21 ± 0.1 (30)	0.57 ± 0.3 (31)	17 ± 17 (33)	78 ± 18 (33)	4.2 ± 10 (33)

[a] The mean and standard deviation are based on a normal distribution which does not fit the distribution of the silt, sand and gravel fraction since these fractions cannot be negative or larger than one. However, this distribution is used to clearly show the difference in variation between the channels.

4.1.3. Large channel

The Large channel was constructed in 1999 and includes a large clay mining pit (Fig. 11). The bed level in this pit goes down to −16 m +NAP (Amsterdam Ordnance Datum), while the bed level in the rest of the channel varies between −2 and +2 m +NAP. At the entrance of the channel the flow velocities are high, but the scour is limited due to the clay layer. The bridge limits the discharge through the Large channel and thereby creates a backwater effect in the upstream part of the channel that reduces the flow velocity. This resulted in aggradation in the upstream part of the Large channel. Below and downstream of the bridge large flow velocities occur due to the small channel width below the bridge. The bed below the bridge is protected and this leads to a large sediment transport capacity, but a limited sediment transport. This leads to large scour just downstream of the bridge (−10 m +NAP). Due to the widening of the channel, the flow quickly decelerates and the sediment that was eroded from the scour hole formed a small island. The bed level of 2009 shows that the mining pit was filled with sediment and to deliver this sediment to the side channel a small channel was dredged. It is likely that the sediment samples that were collected in the downstream part of the Large channel were affected by this intervention. The measurements of 2018 show that the dredged channel was partly refilled with sediment and the bed level in the mining pit has continued to increase. In the downstream part of the Large channel between the islands, the aggradation is limited between 2001 and 2009. This is a result of low flow velocities and a limited sediment supply, because most of the sediment was deposited in the mining pit.

4.2. Grain sizes in the top layer

We measured the grain size in the three side channels and first only present the samples collected in 2017 (Table 2). The average D_{10} in the Large channel is slightly overestimated, because the samples in which the silt/clay fraction is larger than 10% are not included here. The percentage of silt in the Large channel is much larger than in the other channels. The variation in grain size is also largest in the Large channel and this seems to be caused by the variation in width and the bridge that cause large gradients in the bed shear stress.

Both the West and the East channels are mainly filled with sand. The sand that is deposited in the East and West channels is only in a small fraction present on the bed of the main channel. The D_{50} in

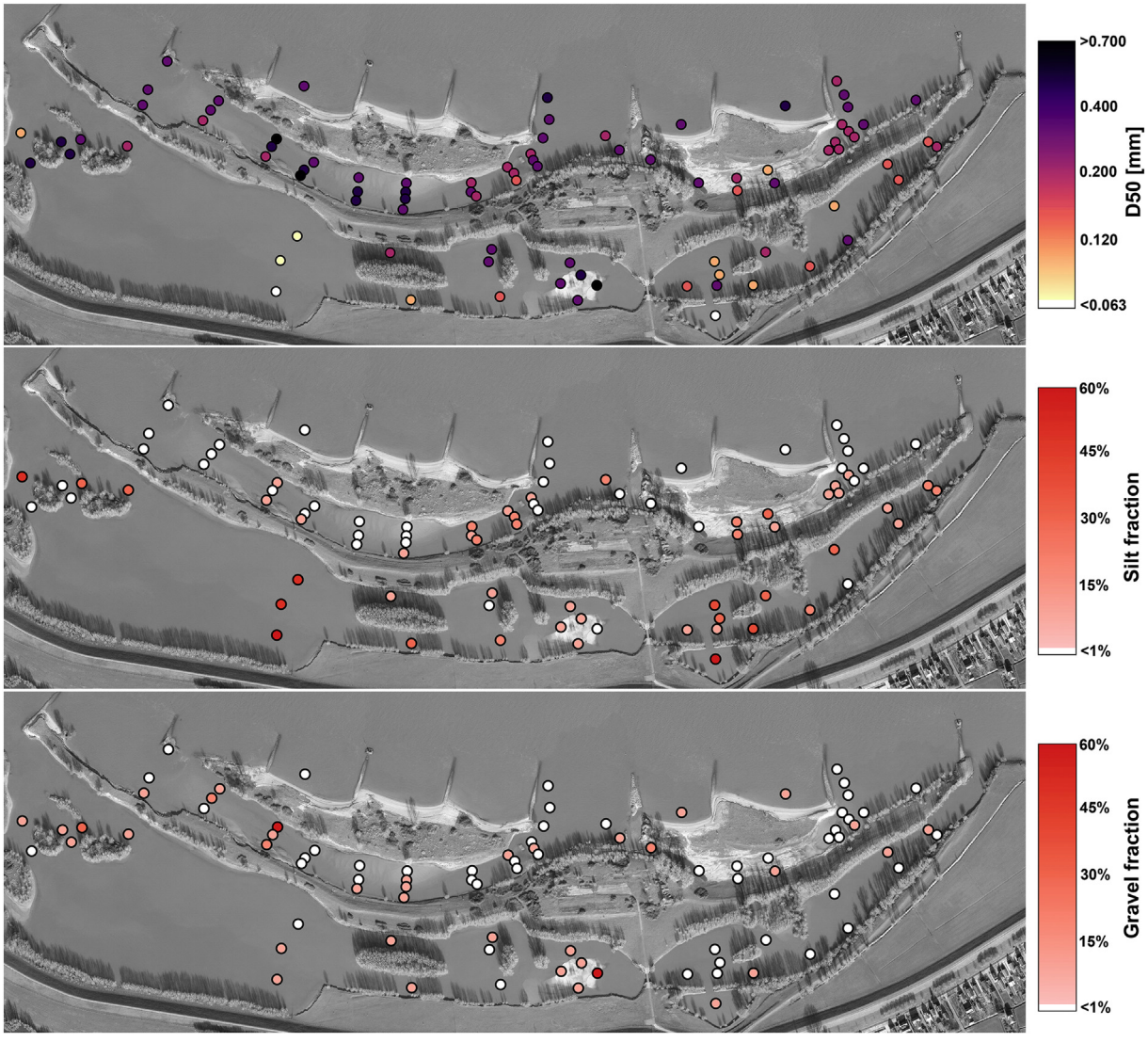

Fig. 12. The spatial variation of the D_{50}, the silt/clay fraction, and the gravel fraction in the three side channels at Gameren.

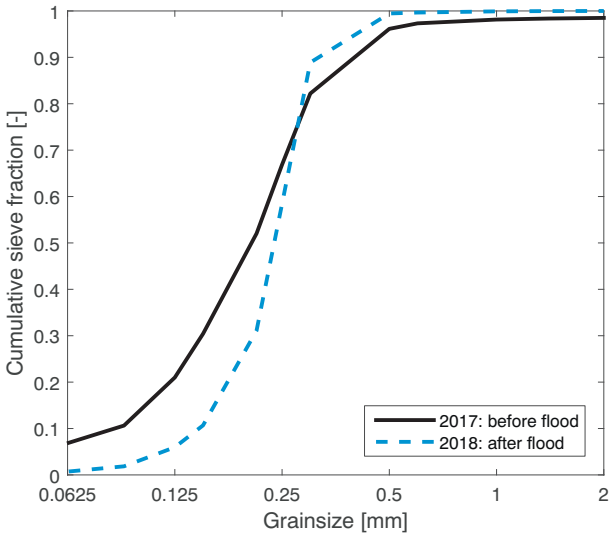

Fig. 13. Comparison of the grain size in the East channel from 2017 before the peak flow and from 2018 after the peak flow.

the East and West channel is similar to the suspended bed-material load at the Pannerdensche Kop and the Merwede Kop during peak flows (Figs. 1 and 3). Apparently, the suspended bed-material load in the main channel enters the side channels and is transported inside the channels as bedload. The sand deposited in the Large channel also corresponds with the suspended bed-material load in the main channel, but here also a large fraction of silt is found that in the main channel is transported as suspended load.

In the East channel, additional samples were collected of the sediment that was deposited during the peak flow in 2018 (5050 m^3/s). A sand layer was deposited on top of the loamy sand layer that was found in 2017 (Fig. 13). The deposited sediment is unimodal and comparable with the sand size previously found in the East channel. However, the silt fraction is much smaller and it seems likely that silt was deposited during the long period of low discharge before the 2017 measurement.

4.3. Sediment cores in the East and West channels

Several sediment cores were taken upstream and downstream of the weir in the East channel (Fig. 14A). The deeper cores are affected by the original clay layer and are excluded from the statistical analysis. The graphs show a fining upward sequence except for D_{10} downstream of the weir. The sediment that was deposited in the East channel was apparently initially coarser and with the increasing bed level the grain size decreases. The sediment supply to the channel becomes finer with increasing bed level, because fine sediment is transported up a bed slope more easily (Parker and Andrews, 1985). The transport capacity in the channel is reduced due to the lower bed shear stress (Fig. 16). The D_{10} and D_{50} do not show a clear difference upstream and downstream of the weir. For the D_{90}, the increase of the grain size with increasing distance below the bed level is larger upstream of the weir compared to downstream of the weir. The largest particles were blocked by the weir during the initial aggradation causing more coarse sediment to be deposited upstream of the weir compared to downstream of the weir. With increasing bed level upstream of the weir and lower bed shear stresses, the supply and thereby the deposition of coarse sediment upstream of the weir

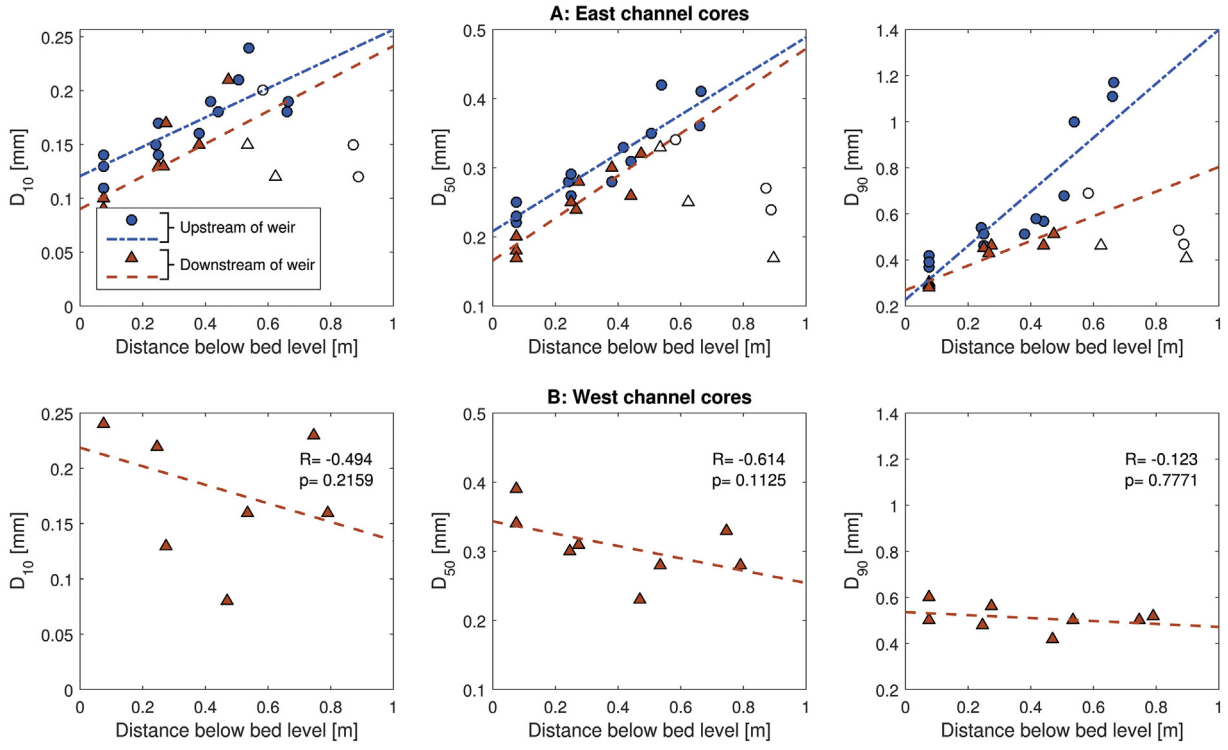

Fig. 14. (A) The depth of the grain size samples compared to the grain size at the upstream and downstream side of the weir in the East channel. The markers without filling are samples that are likely affected by the initial clay layer and are therefore excluded from the correlation analysis. (B) The depth of the grain size samples compared to the grain size in the point bar of the West channel. The locations of the sediment cores are shown in Fig. 1.

decreased. In 2017, the bed level upstream of the weir and downstream of the weir was the same as the weir height and therefore the grain size was very similar in front and behind the weir.

The cores show that the sediment in the lower layers in the East channel is similar to the sediment that is currently found in the top layer of the West channel. In the point bar of the West channel, two cores were taken that do not show a clear trend in the grain size over the depth (Fig. 14B). The grain size that was deposited in the West channel seems therefore constant in time. Initially, sediment deposited in the East and West channel was therefore more similar. The bed level increase and the decrease of the bed shear stress in the East channel resulted in a decrease of the D_{50}. In the West channel, the transport capacity has not decreased sufficiently such that fining of the bed occurs.

4.4. Hydrodynamic results

The hydrodynamic model result shows that the discharge in the side channels has generally decreased due to the bed level changes in these channels (Fig. 6). In the Large channel the initial bed level changes that occurred at the entrance of the side channel results in an increase of the discharge through the channel. The discharge is not constant over the length of each channel (Fig. 15). At $Q = 4000\ m^3/s$ a part of the discharge flows back from the East channel to the main channel and at $Q = 5000\ m^3/s$ a part of the discharge flows from the East and West channel to the Large channel. In addition, at $Q = 4000\ m^3/s$ a part of the discharge enters the Large channel from the upstream floodplain (Fig. 15).

The exchange of discharge between the channels and the floodplain affects the bed shear stress in the channels and therefore the sediment transport capacity (Fig. 16). The bed shear stress increases with increasing discharge until exchange between the floodplain and other channels occurs. Over time, the bed shear stress in the West and Large channels has decreased. This is a result of bed level changes in the side channels which lead to, among other things, a reduction of the discharge conveyance. In the East channel, the bed shear stress increased between 1996 and 1999. At the entrance of the East channel, the channel is narrow resulting in large the bed shear stresses, and due to the bank erosion that occurred in this period the discharge conveyance of the channel increased (Fig. 6). With the continuing bank erosion and aggradation of the channel, the bed shear stress decreases between 1999 and 2017 (Fig. 16).

4.5. Relation between the measurements and the model results

4.5.1. Bed level

We compute the average bed level change over the length of the East and the West channel (Fig. 17). The Large channel is not included

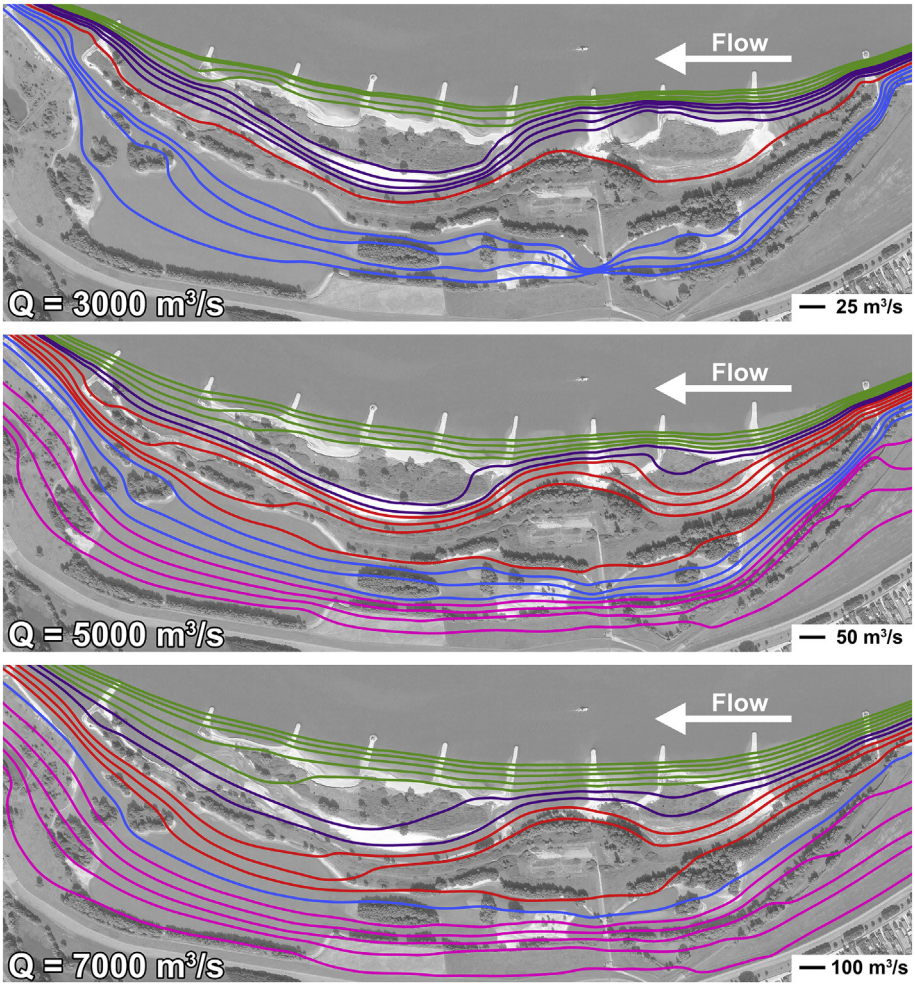

Fig. 15. The streamlines in the side channel system near Gameren based on the depth-averaged hydrodynamic computations for three upstream discharges in the river Waal. The colors of the lines categorize the channel based on the location where they enter the floodplain. Pink lines enter the floodplain upstream of the side channel system, blue lines at the entrance of the Large channel, red lines at the entrance of the East channel, purple lines at the entrance of the West channel and green lines do not enter the floodplain. (Background: Google Earth).

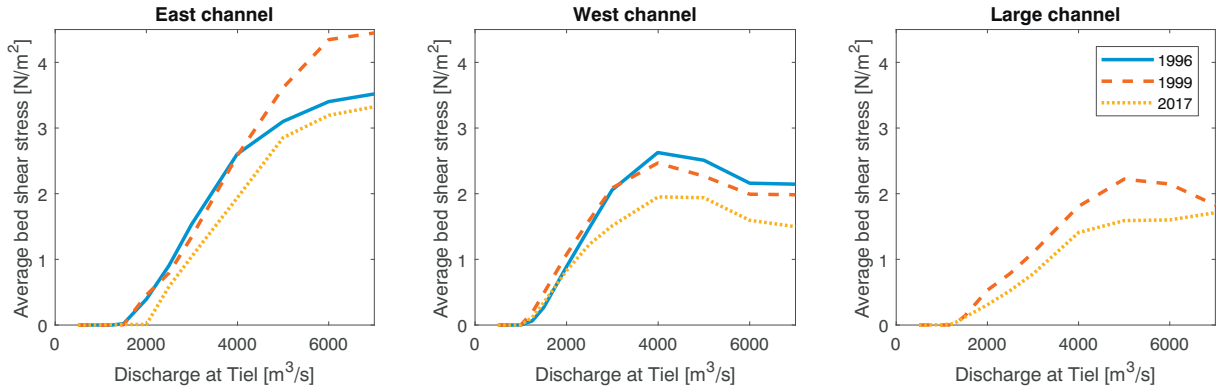

Fig. 16. The average bed shear stress on the center line of the three channels for the bed level in 1996, 1999 and 2017. The discharge in the main channel ranges between 500 m^3/s and 7000 m^3/s.

because we have insufficient data, and in the downstream part of the Large channel, the bed level changes are strongly affected by the dredging and sediment dumping around 2009. In both the West and the East channel, the initial aggradation rate was large, and between 2000 and 2003 the bed level decreased. The bed level again increased in both channels after 2003, but the aggradation rates vary in time. On average, the bed level changes in the East channel seem to follow an exponential function (Fig. 17B). An exponential function seems reasonable because the initial bed level change is large and with increasing bed level the sediment supply is expected to decrease until it reaches a bed level height from which much smaller floodplain aggradation rates occur (Riquier et al., 2017; Van Denderen et al., 2018a). The exponential function suggests that this bed level height is reached when the bevel change is between 1.3 and 1.4 m

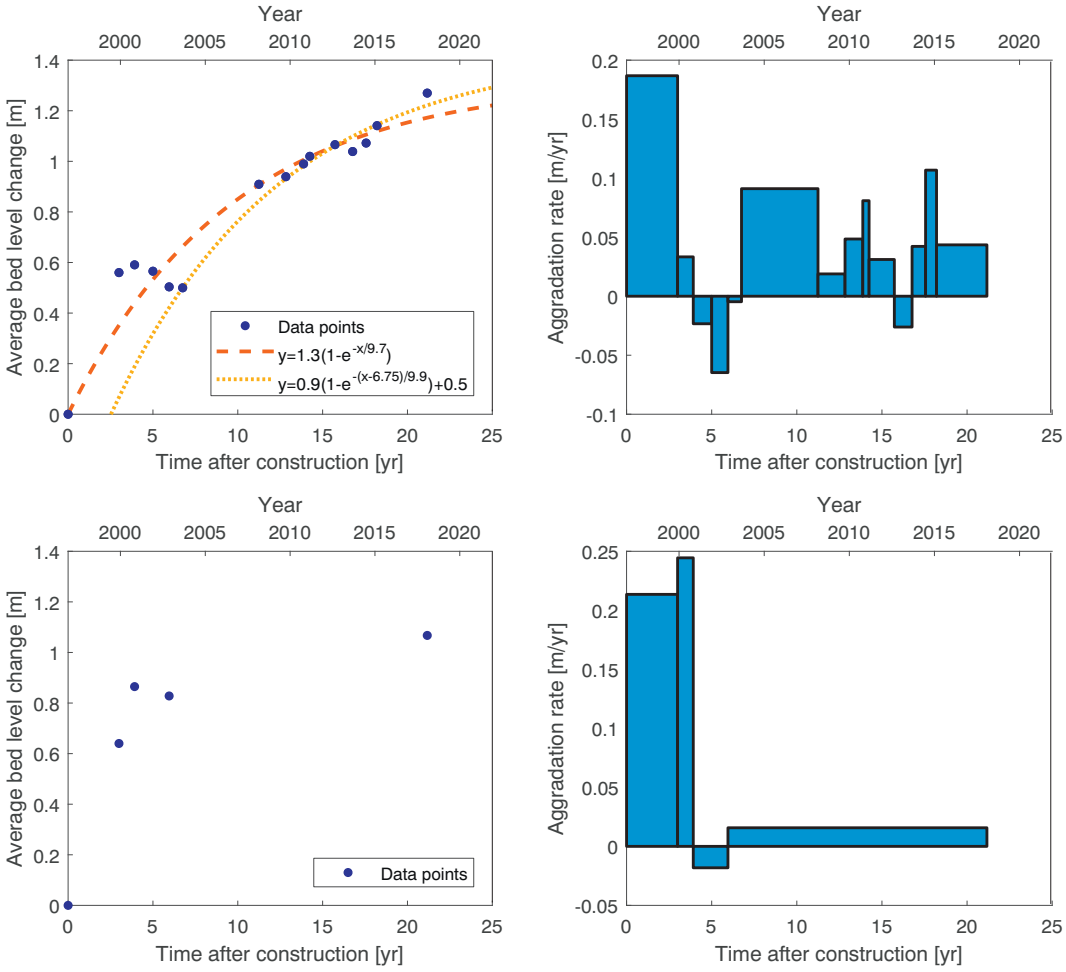

Fig. 17. (A) The mean bed level change of the center line of the East channel (Fig. 7) versus the number of years after construction. An exponential curve is fitted for the starting condition in 1996 and 2003 (Riquier et al., 2017; Van Denderen et al., 2018a). (B) The average aggradation rate of the East channel between each measurement. (C) The mean bed level change of the center line of the West channel versus the number of years after construction. (D) The average aggradation rate of the West channel between each measurement.

(Fig. 17). However, the aggradation rates of the side channel have not yet decreased significantly and therefore this bed level change is likely underestimated.

The aggradation rates vary due to the hydrodynamic conditions of the river and in the side channels (Fig. 18). We compare the bed level changes in the East channel to the hydrodynamic conditions of the river. We ignore the initial bed level change, i.e., the change between 1996 and 1999, because this bed level change is dominated by the migration of the aggradation front. In addition, we scale the hydrodynamic and the bed level changes between measurements to yearly changes, and we therefore do not consider the measurements that are less than 10 months apart because otherwise the hydrodynamic conditions do not represent a full year. We find that the number of days that the East channel conveys discharge is negatively related to the bed level change (Fig. 18A) and this relation is significant ($p<0.01$) using the Spearman's rank correlation. A similar result is found for the cumulative discharge (Fig. 18C). The cumulative discharge is related to the bed shear stresses that occurred in the East channel. Long periods of high water can lead to degradation of the bed in the East channel. The bed shear stress in the East channel is large enough during the large discharges (Fig. 16) such that a part of the deposited sediment is flushed from the channel (Fig. 18D). The peak discharge is not a good predictor for the bed level change (Fig. 18B, $p > 0.01$), which makes sense as it does not include a time duration, which is relevant for the amount of sediment transported and therefore the bed level change. The same holds for the bed shear stress (Fig. 18D).

4.5.2. Grain size

The grain size that is deposited in the side channels is expected to be related to the sediment supply, the bed shear stress and the bed level. The sediment supply to the side channels is difficult to estimate because it is, among other things, a function of local three-dimensional flow patterns (e.g., Dutta et al., 2017). The depth-averaged streamlines (Fig. 15) show that most of the discharge in the East channel comes directly from the main channel. The flow that enters the West channel comes for a large part from the East channel or its floodplain. This could suggest that the West channel receives less sediment since a part of the sediment can settle in the East channel. The size of this effect depends on the sediment exchange that occurs with the main channel in the groyne field at the bifurcation of the West channel, which requires more detailed data to estimate. The Large channel receives discharge from the East channel, the West channel, the main channel and the upstream floodplain. The discharge from the upstream floodplain flows parallel to the main channel and more than 100 m away from the main channel. Therefore, this discharge transports mainly silt/clay (Middelkoop and Asselman, 1998). We expect therefore that the sand supply to the Large channel is relatively small during peak discharges.

The longitudinal profile of the East channel shows that the highest bed level occurs halfway down the channel (Fig. 19). Fig. 20 shows a negative relation between the bed level and the D_{50}. Fine sediment is more easily transported up a bed slope compared to coarser sediment (Parker and Andrews, 1985) and the bed shear

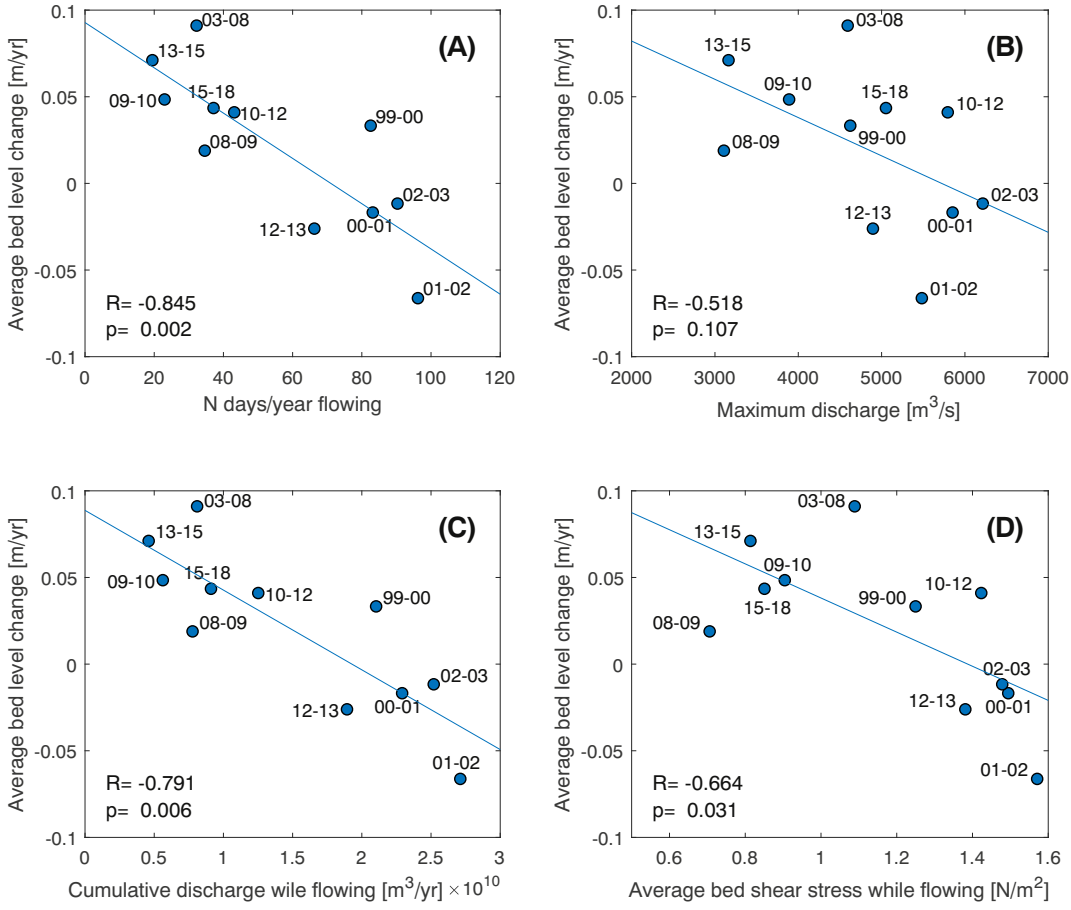

Fig. 18. The correlation between the average bed level change and (A) the average number of days per year that the side channel flows ($Q > 2200\,m^3/s$), (B) the maximum discharge that occurred between each measurement, (C) the yearly averaged cumulative discharge during which the side channel flows between each bed level measurement, and (D) the averaged bed shear stress during which the side channel flows between each bed level measurement based on the hydrodynamic model. The correlation coefficients and the *p*-values are based on a Spearman's rank correlation and the linear regressions are based on a least-square fit.

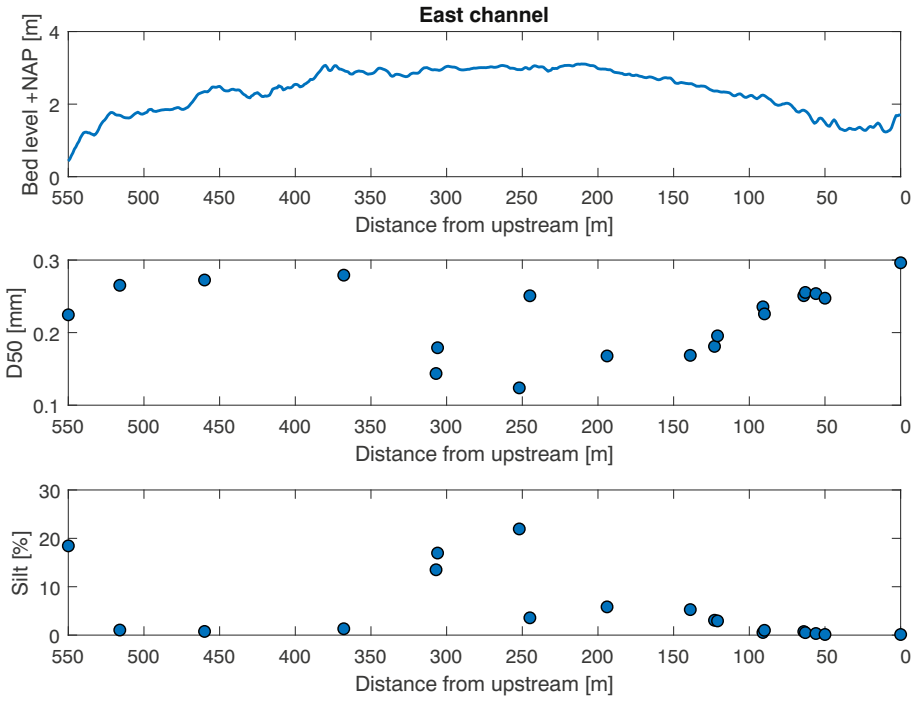

Fig. 19. The bed level (2018), the grain size (2017) and the silt fraction (2017) on the center line of the East channel (Fig. 7).

stress decreases with the increasing bed level (Fig. 16). The silt fraction shows a positive relation with the bed level. The D_{50} decreases and the silt fraction increases from a bed level height of 1.5–2.0 m +NAP (Fig. 20), i.e., in the whole channel except for its extremities. This suggest that from this bed level height the trapping of silt occurs. This is enhanced by the growth of vegetation and the low discharges that occurred in the months before the grain size sampling. The three points above a bed level of 2 m +NAP that are relatively coarse (Fig. 20A) are in the downstream end of the side channel where the channel narrows and therefore higher bed shear stresses occur. The point with the lowest bed level and a high silt fraction (Fig. 20B) is in the downstream groyne field. During base flow conditions, which was the case during the measurements, the flow velocity in the groyne field is low. The main flow is likely directed towards the entrance of the West channel and a flow circulation forms at the upstream side of the groyne field (Mosselman et al., 2004). The low flow velocity in the flow circulation can result in the deposition of fines at the downstream end of the East channel (Sukhodolov et al., 2002).

In the West channel the grain size is on average the largest of the three channels. The weir at the entrance does not block the flow and therefore during base flow conditions the scour hole at the entrance of the channel is filled with fines (Fig. 21). The samples were collected after a long period with lower discharges, and it is therefore likely that during peak flows this deposited fine sediment erodes. In the remaining part of the channel, the silt fraction is small because the flow velocity is sufficiently high that fines do not settle. There is some variation of the D_{50} over the width of the channel (Fig. 12)

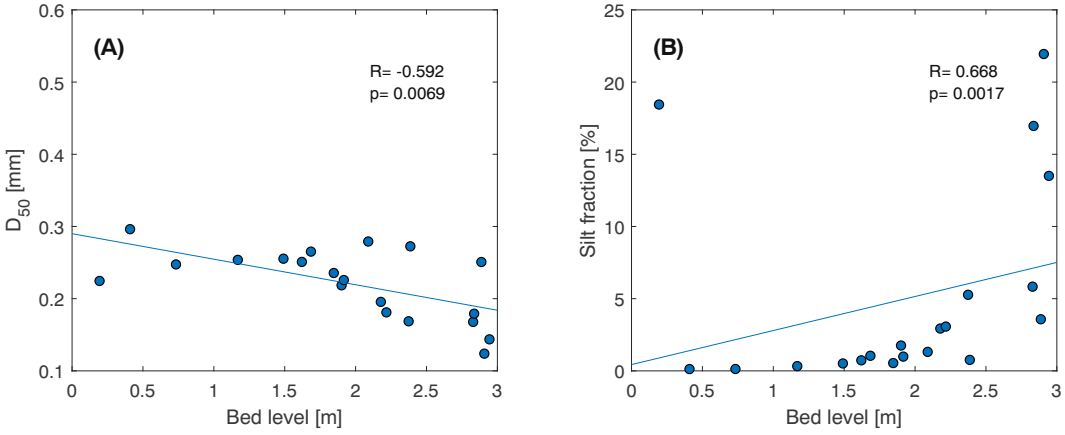

Fig. 20. The D_{50} and the silt fraction in the East channel as a function of the bed level. The correlation coefficients were computed using Spearman's rank correlation and the linear regression is based on a least-square fit.

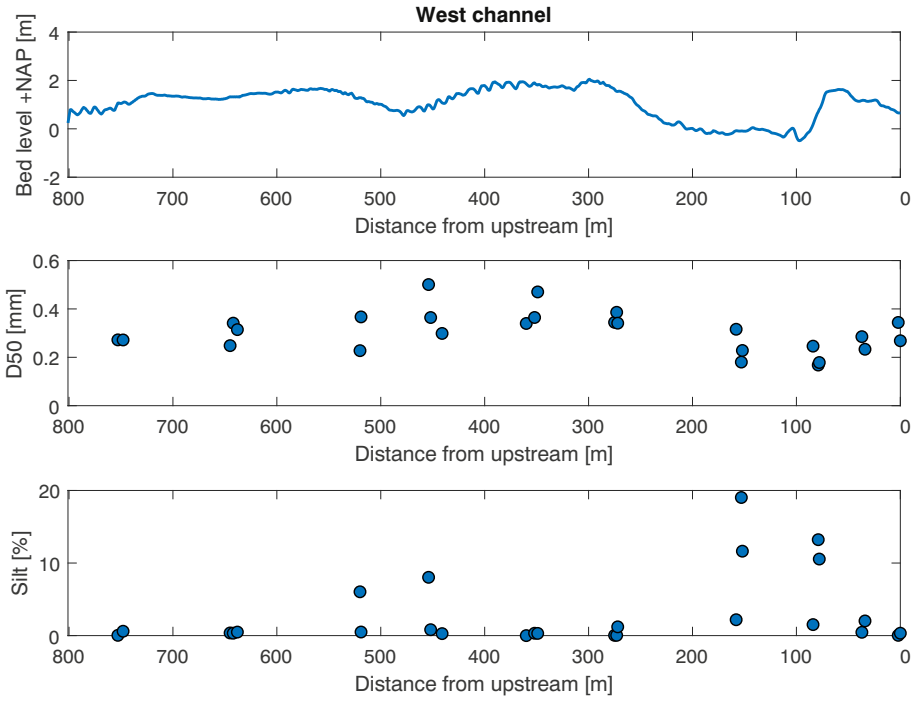

Fig. 21. The bed level (2018), the D_{50} (2017) and the silt fraction (2017) on the center line of the West channel (Fig. 9).

and this is related to the bend in which, due to the transverse bed slope, more fine sediment is deposited in the inner part of the bend (Parker and Andrews, 1985). The D_{50} in the West channel does not show a correlation with the bed shear stress, nor with the bed level (Supplementary material 2), because the bed level of 2.0 m +NAP at which in the East channel fining occurred is not yet reached in this channel. At the downstream end a few samples show a large gravel fraction. Since the gravel is not found in the rest of the channel, this is likely a result of the bank erosion that occurred here (Fig. 5).

The largest silt fraction is found in the Large channel. The threshold value for the bed shear stress below which fines can settle is estimated at around 2.0 N/m^2 for the sediment in the river Waal (Middelkoop and Van der Perk, 1998; Asselman and Van Wijngaarden, 2002). On average, fines can settle in the Large channel even during peak flows (Fig. 16). The large variation of the channel width and depth results in a large variation of the bed shear stress and thereby the D_{50} and the silt fraction (Fig. 22). The thalweg of the Large channel is located next to the south bank upstream of the bridge and downstream of the bridge next to the north bank (Fig. 11). In these areas we find coarser sediment, and the silt/clay fraction is lower than in the rest of the channel. At the entrance of the channel, large flow velocities occur and it was not possible to take a sample with the Van Veen grab. Here, the bed is likely covered with clay that limits the scour at the entrance. The island that formed just downstream of the bridge is partly covered with gravel and this originates from the deep scour hole just downstream of the bridge. The large acceleration at the bridge allows for the pickup of the gravel, but the deceleration just downstream causes it to be deposited. At the downstream end of the channel in between the islands, it is not clear whether the sampled sediment was deposited naturally or dumped due to dredging activities. In addition, the measurements show very limited aggradation and therefore the sediment could have been there since the construction of the channel.

5. Discussion

5.1. Characterization of the side channels at Gameren

The three side channels at Gameren present two types of side channels. The East and West channel are mainly filled with sand from the main channel that in the main channel is transported as suspended bed-material load. The Large channel also shows the deposition of silt in addition to the suspended bed-material load. We expect that the West and East channel show a comparable development and that the difference in aggradation rate is caused by the design conditions of the channels.

Both the East and West channel have a similar relative length compared to the main channel (L_{side}/L_{main}), which was found to have large effect on the time scale of the side channel development (Van Denderen et al., 2018a). The initial bed level changes seem similar (Fig. 17) and the corings in the East channel show that the sediment that was initially deposited in the East channel was similar in size to the sediment currently found in the West channel (Fig. 14). We therefore expect both channels to have a similar equilibrium state, but that the aggradation time scale differs. An important factor is the initial geometry. The West channel is wider compared to the East channel, and the initial bed level and weir height are lower. Therefore, the West channel flows more frequently than the East channel and the aggradation rate is therefore likely smaller compared to the East channel (Fig. 18A). In addition, the sediment supply might differ between the West and the East channel. The flow at the bifurcation of the West channel is affected by the outflow of the East channel (Fig. 15). Based on the 2D hydrodynamic model, a large part of the flow first passes through the East channel before it enters the West channel. This suggests that the East channel can act as a sediment trap for the West channel during peak flow conditions. However, more detailed measurements or computations of the flow velocity in this groyne field are needed to confirm this.

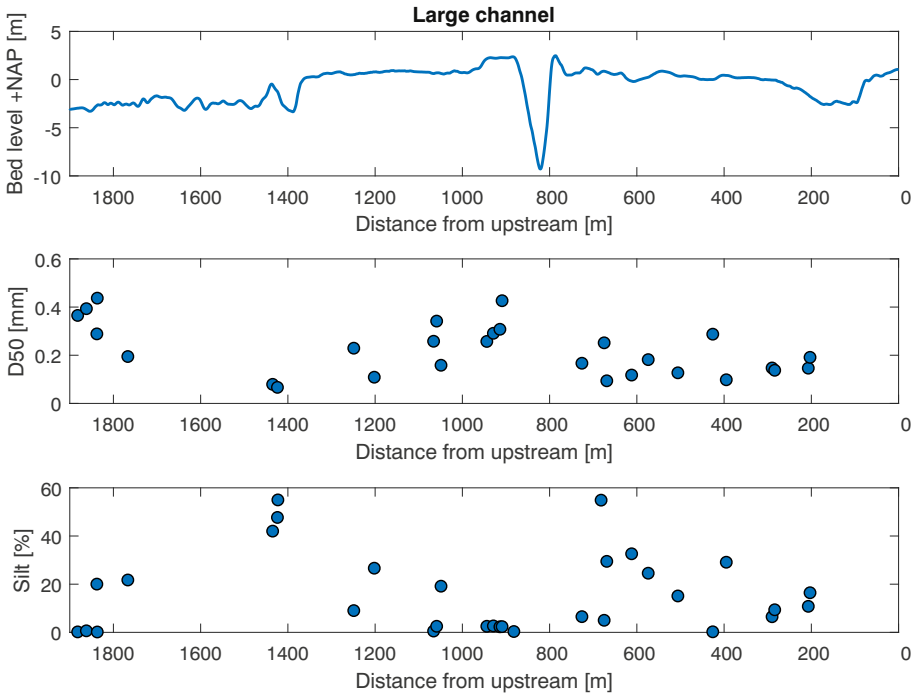

Fig. 22. The variation of the bed level (2009), the D_{50} and the silt fraction on the thalweg of the Large channel (Fig. 11).

The aggradation in the side channels affects the sediment supply and the transport capacity of the channel. The loamy sand layer that was found in the East channel means that fine sediment processes gained importance (Makaske et al., 2002). The aggradation in the East channel has made the channel sufficiently shallow such that vegetation can colonize and trap suspended load. In addition, the loamy sand layer can be a result of a long period of lower discharges that reduced the supply of coarse sediment. The recent peak flow (2018) resulted locally in large amounts of deposition of fine sand in the East channel. Coarser sediment is therefore supplied during peak flow conditions during which larger bed shear stresses occur.

The Large channel belongs to a second type of side channel. The Large channel is much longer than the main channel and, in combination with the large variations in width, this results in areas with small bed shear stresses. In these areas, we found large amounts of silt deposited. In addition, the channel is located in the floodplain and during peak flows, a large part of the flow originates from the floodplain that mainly carries fine sediment. Therefore, the supply of fines to the Large channel during peak flows might be relatively large compared to the supply of suspended bed-material load.

These two types of side channels are similar to the modes of infilling of channels that were found in anabranching rivers (Makaske et al., 2002). The way the channel is filled strongly depends on the sediment supply. The West and the East channel receive sediment that is transported inside the channel as bedload. This leads to a gradual aggradation in the channel until a certain bed level is reached and fines start to be deposited (Makaske et al., 2002; Dieras et al., 2013). The Large channel receives much less sand because it attracts relatively less discharge due to its length (Van Denderen et al., 2018a) and little sediment is supplied from the main channel during peak flows (Fig. 15). This results in the deposition of fines (Makaske et al., 2002), which is similar to the aggradation in oxbow lakes (Constantine et al., 2010; Toonen et al., 2012).

5.2. Knowledge gaps

In the Room for the River program in the Netherlands, over 20 side channels were constructed since 1996. Unfortunately, the monitoring of these side channels was limited except for Gameren. Therefore, the side channels at Gameren provide a unique opportunity to study the development of side channels in the Dutch Rhine branches. In this paper, a range of measuring techniques is used to characterize the sediment dynamics. Each technique has its limitations and inaccuracies. The regular LIDAR measurements between 2008 and 2015 provide insight into the development of the East channel. Unfortunately, the West and Large channel are permanently inundated and therefore aerial height measurements cannot give accurate information on the bed level changes in these channels.

In this paper, we mainly focus on the mechanisms that are not human-induced. However, there are several human-induced changes that might have influenced the development of the side channels. Between 2013 and 2014, the groyne height in the main channel was reduced over a large stretch. This led to higher flow velocities in the groyne field (Yossef, 2005) and a lower bed level (Klop and Dongen, 2015). This likely produces an increased sediment supply to the side channels because the larger bed shear stress allows for more sediment to be transported up a sloping bed (Parker and Andrews, 1985). The bed level of 2018 deviates from the proposed exponential function (Fig. 17) and this might be due to the changed sediment supply during peak flows. Unfortunately, this cannot be confirmed because of the limited frequency of bed level measurements in the more recent years. A second example of human impacts are navigation-induced currents. Navigation in the main channel causes an export of sediment from the groyne fields (Ten Brinke et al., 2004). The currents likely have a similar effect at the entrances of the side channels. For example, the bed level at the bifurcation of the East channel in 2018 is much higher than in the other years (Fig. 8). These measurements were collected during the peak flow in 2018 and therefore navigation had a limited effect on the bed level.

All the other measurements were carried out at the beginning of the flood season, and therefore navigation-induced currents might have reduced the bed level at the entrance of the East channel. In addition, it is possible that during base flow conditions fine sediments are supplied to the channels due to the navigation-induced currents. Vessels that pass through the main channel cause a depression of the water level in the side channel, and after the vessel passes the water level rises again. This water level variation is enough to bring fine sediment into suspension (Ten Brinke et al., 2004) and might therefore lead to aggradation of the channel. Especially in the Large channel, which is continuously connected with the main channel and in which the bed shear stress is generally low (Fig. 16), this can result in the deposition of fines.

Besides the groyne field dynamics, the bed level changes and the aggradation rates of the side channels are also related to the flow conditions in the main channel (Figs. 17 and 18). Just after the construction of the side channel system several large peak discharges occurred, but during other periods, e.g., 2004–2010, the flood frequency was much lower (Fig. 2). The duration needed to fill in a side channel will increase with regular large peak discharges (Fig. 18).

6. Conclusion

The three side channels near Gameren all show aggradation after their construction. The East and West channels are very similar in terms of sediment dynamics. In both channels large aggradation occurred and mainly sand was deposited. The aggradation rate of the East channel shows a relation to the hydrodynamic conditions of the river. The measurements show that a more frequent flowing side channel results in lower aggradation rates. The aggradation in the East channel was large enough such that vegetation has grown and silt has deposited. The East channel is therefore slowly becoming a part of the floodplain. The aggradation in the West channel initially reacts to hydrodynamic events similarly to the East channel. The aggradation rate in the West channel is slower after the initial 5 yr after construction, but the bed level continues to increase and we expect that the bed level will continue to increase until it reaches a similar bed level as the East channel. The smaller aggradation rate of the West channel seems to be related to a different initial geometry, which allows the channel to flow more frequently compared to the East channel, and a difference in sediment supply compared to the East channel. The West channel is located just downstream of the East channel and might therefore receive a smaller sediment supply.

The aggradation of the Large channel was different than that of the other two channels. The length of the channel is much larger than the length of the main channel and in combination with variation in channel width this results in areas with low bed shear stresses. In addition to suspended bed-material load, silt is deposited in the Large channel due to the low bed shear stresses. During peak flows a large part of the discharge in the Large channel originates from the floodplain and therefore mainly carries fines. The supply of sand to the channel relative to the discharge in the channel is therefore likely lower during peak flows and this reduces the aggradation rate.

Acknowledgments

This research is supported by the Netherlands Organisation for Scientific Research (NWO), which is partly funded by the Ministry of Economic affairs, under grant number P12-P14 (RiverCare Perspective Programme) project number 13516. This research has benefited from cooperation within the network of the Netherlands Centre for River studies. Datasets related to this article can be found at https://doi.org/10.4121/uuid:2704f813-d23b-43b5-b837-fdb02ceef261, hosted at 4TU.Centre for Research Data (Van Denderen et al., 2018b). We thank Anouk Bomers for her help in setting up and calibrating the hydrodynamic numerical model. The Editor Scott Lecce and three anonymous reviewers are acknowledged for their valuable comments that helped to improve the paper.

Appendix A. Supplementary data

Supplementary data to this article can be found online at https://doi.org/10.1016/j.geomorph.2018.10.016.

References

Akkerman, G., 1993. Zandverdeling bij splitsingspunten: Literatuurinventarisatie voor inlaten van nevengeulen. Technical Report Q1573, WL Delft Hydraulics, Delft, The Netherlands.

Asselman, N.E.M., Van Wijngaarden, M., 2002. Development and application of a 1D floodplain sedimentation model for the river Rhine in the Netherlands. J. Hydrol. 268, 127–142. https://doi.org/10.1016/S0022-1694(02)00162-2.

Baptist, M., Mosselman, E., 2002. Biogeomorphological modelling of secondary channels in the Waal River. In: Bousmar, D., Zech, Y. (Eds.), Riverflow 2002, Proceedings of the International Conference on Fluvial Hydraulics. Louvain-la-Neuve, Belgium., pp. 773–782.

Becker, A., Scholten, M., Kerhoven, D., Spruyt, A., 2014. Das behördliche Modellinstrumentarium der Niederlande. Dresdner Wasserbauliche Mitteilungen 50. pp. 539–548.

Bolla Pittaluga, M., Repetto, R., Tubino, M., 2003. Channel bifurcation in braided rivers: equilibrium configurations and stability. Water Resour. Res. 39, https://doi.org/10.1029/2001WR001112.

Bulle, H., 1926. Untersuchungen über die Geschiebeableitung bei der Spaltung von Wasserläufen. VDIVerlag, Berlin, Germany.

Citterio, A., Piégay, H., 2009. Overbank sedimentation rates in former channel lakes: characterization and control factors. Sedimentology 56, 461–482. https://doi.org/10.1111/j.1365-3091.2008.00979.x.

Constantine, J.A., Dunne, T., Piégay, H., Kondolf, G.M., 2010. Controls on the alluviation of oxbow lakes by bed-material load along the Sacramento River, California. Sedimentology 57, 389–407. https://doi.org/10.1111/j.1365-3091.2009.01084.x.

De Vries, M., 1971. Aspecten van zandtransport in open waterlopen. Technical Report, Delft University of Technology, Delft, The Netherlands.

Dieras, P.L., Constantine, J.A., Hales, T.C., Piégay, H., Riquier, J., 2013. The role of oxbow lakes in the off-channel storage of bed material along the Ain River, France. Geomorphology 188, 110–119. https://doi.org/10.1016/j.geomorph.2012.12.024.

Dutta, S., Wang, D., Tassi, P., Garcia, M.H., 2017. Three-dimensional numerical modeling of the Bulle effect: the nonlinear distribution of near-bed sediment at fluvial diversions. Earth Surf. Process. Landf. 42, 2322–2337. https://doi.org/10.1002/esp.4186.

Formann, E., Habersack, H.M., Schober, S., 2007. Morphodynamic river processes and techniques for assessment of channel evolution in Alpine gravel bed rivers. Geomorphology 901, 340–355. https://doi.org/10.1016/j.geomorph.2006.10.029.

Frings, R.M., 2007. From Gravel to Sand. PhD thesis. University of Utrecht, Utrecht, The Netherlands.

Frings, R.M., Banhold, K., Evers, I., 2015. Sedimentbilanz des oberen rheindeltas. Technical Report, Lehrstuhl und Institut für Wasserbau und Wasserwirtschaft, RWTH Aachen University, Aachen, Germany.

Frings, R.M., Kleinhans, M.G., 2008. Complex variations in sediment transport at three large river bifurcations during discharge waves in the river Rhine. Sedimentology 55, 1145–1171. https://doi.org/10.1111/j.1365-3091.2007.00940.x.

Goodman, S., 2001. Of P-values and Bayes: a modest proposal. Epidemiology 12, 295–297. https://doi.org/10.1097/00001648-200105000-00006.

Hegnauer, M., Beersma, J.J., Van den Boogaard, H.F.P., Buishand, T.A., Passchier, R.H., 2014. Generator of Rainfall and Discharge Extremes (GRADE) for the Rhine and Meuse Basins. Technical Report, Deltares, Delft, The Netherlands.

Hohensinner, S., Jungwirth, M., Muhar, S., Schmutz, S., 2014. Importance of multidimensional morphodynamics for habitat evolution: Danube River 1715–2006. Geomorphology 215, 3–9. https://doi.org/10.1016/j.geomorph.2013.08.001.

Jans, L., 2004. Evaluatie nevengeulen Gamerensche Waard 1996–2002. Technical Report, Rijkswaterstaat, Lelystad, The Netherlands.

Jansen, P., Van Bendegom, L., Van den Berg, J., De Vries, M., Zanen, A., 1979. Principles of River Engineering: The Non-Tidal Alluvial River. Pitman, London.

Kernkamp, H.W.J., Van Dam, A., Stelling, G.S., De Goede, E.D., 2011. Efficient scheme for the shallow water equations on unstructured grids with application to the continental shelf. Ocean Dyn. 61, 1175–1188. https://doi.org/10.1007/s10236-011-0423-6.

Kleinhans, M.G., de Haas, T., Lavooi, E., Makaske, B., 2012. Evaluating competing hypotheses for the origin and dynamics of river anastomosis. Earth Surf. Process. Landf. 37, 1337–1351. https://doi.org/10.1002/esp.3282.

Kleinhans, M.G., Ferguson, R.I., Lane, S.N., Hardy, R.J., 2013. Splitting rivers at their seams: bifurcations and avulsion. Earth Surf. Process. Landf. 38, 47–61. https://doi.org/10.1002/esp.3268.

Kleinhans, M.G., Jagers, H.R.A., Mosselman, E., Sloff, C.J., 2008. Bifurcation dynamics and avulsion duration in meandering rivers by one-dimensional and three-dimensional models. Water Resour. Res. 44, https://doi.org/10.1029/2007WR005912.

Klop, E., 2015. Morfologische ontwikkeling hoofd- en vaargeul na kribverlaging op basis van multibeamgegevens in periode 2009–2012. Technical Report, Arcadis, Amersfoort, The Netherlands.

Klop, E., Dongen, B., 2015. Morfologische dynamiek in kribvakken na kribverlaging. Technical Report, Arcadis, Amersfoort, The Netherlands.

Makaske, B., Smith, D.G., Berendsen, H.J.A., 2002. Avulsions, channel evolution and floodplain sedimentation rates of the anastomosing upper Columbia River, British Columbia, Canada. Sedimentology 49, 1049–1071. https://doi.org/10.1046/j.1365-3091.2002.00489.x.

Mendoza, A., Abad, J.D., Frias, C.E., Ortals, C., Paredes, J., Montoro, H., Vizcarra, J., Simon, C., Soto-Cortes, G., 2016. Planform dynamics of the Iquitos anabranching structure in the Peruvian Upper Amazon River. Earth Surf. Process. Landf. 41, 961–970. https://doi.org/10.1002/esp.3911.

Middelkoop, H., Asselman, N.E.M., 1998. Spatial variability of floodplain sedimentation at the event scale in the Rhine-Meuse delta, The Netherlands. Earth Surf. Process. Landf. 23, 561–573. https://doi.org/10.1002/(sici)1096-9837(199806)23:6<561::aid-esp870>3.0.co;2-5.

Middelkoop, H., Van der Perk, M., 1998. Modelling spatial patterns of overbank sedimentation on embanked floodplains. Geogr. Ann. Ser. B 80, 95–109. https://doi.org/10.1111/j.0435-3676.1998.00029.x.

Mosselman, E., 2001. Morphological development of side channels. Technical Report, WL Delft Hydraulics, Delft, The Netherlands.

Mosselman, E., Jagers, B., Van Schijndel, S., 2004. Optimalisatie inlaat nevengeulen. Technical Report Q3553, WL Delft hydraulics, Delft, The Netherlands.

Nabet, F., 2014. Etude du réajustement du lit actif en Loire moyenne, bilan géomorphologique et diagnostic du fonctionnement des chanaux secondaires en vue d'une gestion raisonnée. PhD thesis. Université Panthéon-Sorbonne - Paris I, Paris, France.

Nuzzo, R., 2014. Scientific method: statistical errors. Nature 506, 150–152. https://doi.org/10.1038/506150a.

Parker, G., Andrews, E., 1985. Sorting of bed load sediment by flow in meander bends. Water Resour. Res. 21, 1361–1373. https://doi.org/10.1029/WR021i009p01361.

Riquier, J., Piégay, H., Lamouroux, N., Vaudor, L., 2017. Are restored side channels sustainable aquatic habitat features? Predicting the potential persistence of side channels as aquatic habitats based on their fine sedimentation dynamics. Geomorphology 295, 507–528. https://doi.org/10.1016/j.geomorph.2017.08.001.

Riquier, J., Piégay, H., Michalkova, M.S., 2015. Hydromorphological conditions in eighteen restored floodplain channels of a large river: linking patterns to processes. Freshw. Biol. 60, 1085–1103. https://doi.org/10.1111/fwb.12411.

Schiemer, F., Baumgartner, C., Tockner, K., 1999. Restoration of floodplain rivers: the Danube restoration project. Regul. Rivers: Res. Manage. 15, 231–244. https://doi.org/10.1002/(SICI)1099-1646(199901/06)15:1/3<231::AID-RRR548>3.0.CO;2-5.

Sieben, J., 2009. Sediment management in the Dutch Rhine branches. Int. J. River Basin Manage. 17, 43–53. https://doi.org/10.1080/15715124.2009.9635369.

Simons, J.H.E.J., Bakker, C., Schropp, M.H.I., Jans, L.H., Kok, F.R., Grift, R.E., 2001. Man-made secondary channels along the river Rhine (The Netherlands); results of post-project monitoring. Regul. Rivers: Res. Manage. 17, 473–491. https://doi.org/10.1002/rrr.661.

Sorber, A., 1997. Oeversedimentatie tijdens de hoogwaters van 1993/1994 en 1995. Technical Report RIZA 97.015, Rijkswaterstaat, Lelystad, The Netherlands.

Sukhodolov, A., Uijttewaal, W.S., Engelhardt, C., 2002. On the correspondence between morphological and hydrodynamical patterns of groyne fields. Earth Surf. Process. Landf. 27, 289–305. https://doi.org/10.1002/esp.319.

Ten Brinke, W.B.M., 1997. De bodemsamenstelling van Waal en IJssel in de jaren 1966, 1976, 1984 en 1995. Technical Report, Rijkswaterstaat report 97.009, Arnhem, The Netherlands.

Ten Brinke, W.B.M., Schoor, M.M., Sorber, A.M., Berendsen, H.J.A., 1998. Overbank sand deposition in relation to transport volumes during large-magnitude floods in the Dutch sand-bed Rhine river system. Earth Surf. Process. Landf. 23, 809–824. https://doi.org/10.1002/(sici)1096-9837(199809)23:9<809::aid-esp890>3.0.co;2-1.

Ten Brinke, W.B.M., Schulze, F.H., Van der Veer, P., 2004. Sand exchange between groyne-field beaches and the navigation channel of the Dutch Rhine: the impact of navigation versus river flow. Earth Surf. Process. Landf. 20, 899–928. https://doi.org/10.1002/rra.809.

Toonen, W.H.J., Kleinhans, M.G., Cohen, K.M., 2012. Sedimentary architecture of abandoned channel fills. Earth Surf. Process. Landf. 37, 459–472. https://doi.org/10.1002/esp.3189.

Van Denderen, R.P., Schielen, R.M.J., Blom, A., Hulscher, S.J.M.H., Kleinhans, M.G., 2018a. Morphodynamic assessment of side channel systems using a simple one-dimensional bifurcation model and a comparison with aerial images. Earth Surf. Process. Landf. 43, 1169–1182. https://doi.org/10.1002/esp.4267.

Van Denderen, R.P., Schielen, R.M.J., Westerhof, S.G., Quartel, S., Hulscher, S.J.M.H., 2018b. Replication Dataset: Explaining Artificial Side Channel Dynamics Using Data Analysis and Model Calculations. 4TU.Centre for Research Data [dataset]. https://doi.org/10.4121/uuid:2704f813-d23b-43b5-b837-fdb02ceef261.

Van Dyke, C., 2016. Nature's complex flume - using a diagnostic state-and-transition framework to understand post-restoration channel adjustment of the Clark Fork River, Montana. Geomorphology 254, 1–15. https://doi.org/10.1016/j.geomorph.2015.11.007.

Yossef, M.F.M., 2005. Morphodynamics of Rivers with Groynes.PhD thesis. Delft University of Technology, Delft, The Netherlands.

Zinger, J.A., Roads, B.L., Best, J.L., Johnson, K.K., 2013. Flow structure and channel morphodynamics of meander bend chute cutoffs: a case study of the Wabash River, USA. J. Geophys. Res. Earth Surf. 118 (4), 2468–2487. https://doi.org/10.1002/jgrf.20155.